ISSN 0711-6659

canadian acoustics
acoustique canadienne

Journal of the Canadian Acoustical Association - Revue de l'Association canadienne d'acoustique

JUNE 2022	JUIN 2022
Volume 50 - - Number 2	Volume 50 - - Numéro 2

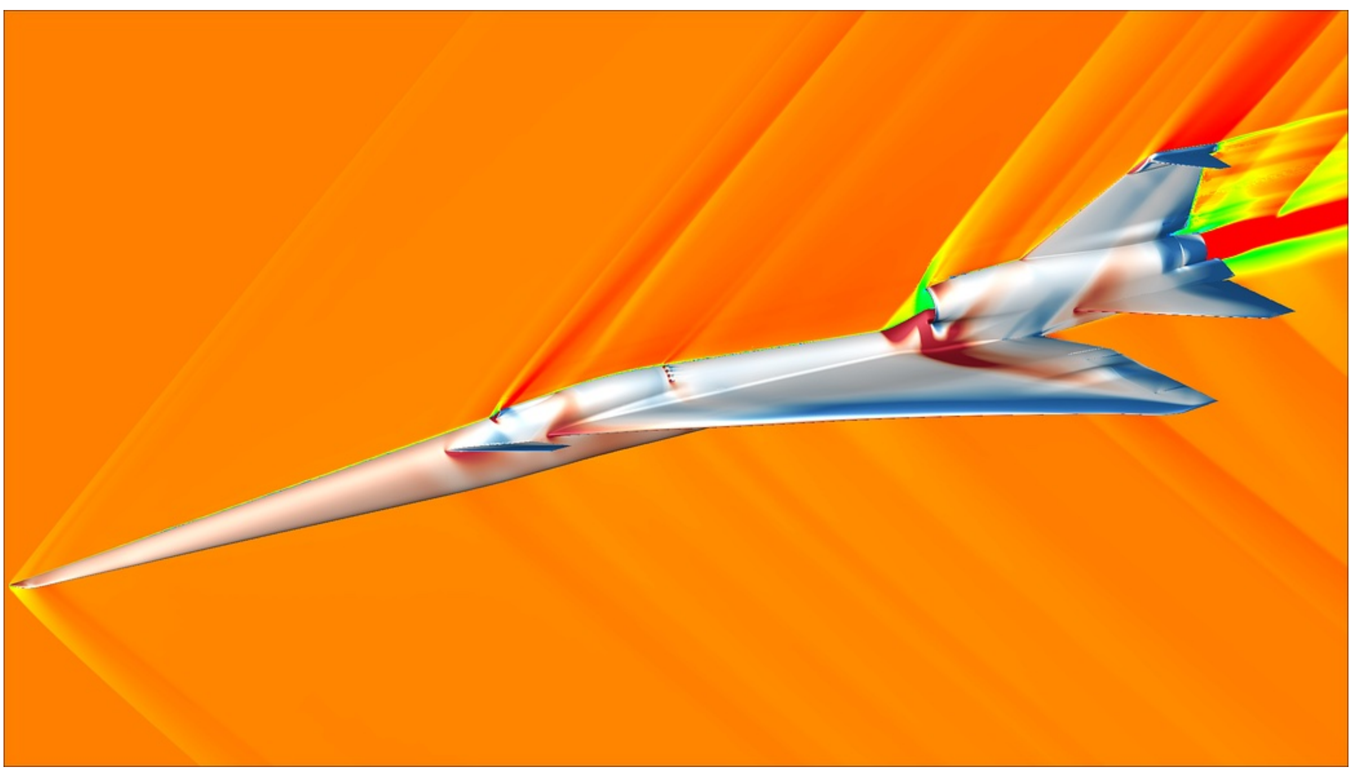

canadian acoustics

acoustique canadienne

Canadian Acoustical Association/Association Canadienne d'Acoustique P.B. 74068 Ottawa, Ontario, K1M 2H9

Association canadienne d'acoustique B.P. 74068 Ottawa, Ontario, K1M 2H9

Canadian Acoustics publishes refereed articles and news items on all aspects of acoustics and vibration. Articles reporting new research or applications, as well as review or tutorial papers and shorter technical notes are welcomed, in English or in French. Submissions should be sent only through the journal online submission system. Complete instructions to authors concerning the required "camera-ready" manuscript are provided within the journal online submission system.

L'**Acoustique Canadienne** publie des articles arbitrés et des informations sur tous les aspects de l'acoustique et des vibrations. Les informations portent sur la recherche, les ouvrages sous forme de revues, les nouvelles, l'emploi, les nouveaux produits, les activités, etc. Des articles concernant des résultats inédits ou des applications ainsi que les articles de synthèse ou d'initiation, en français ou en anglais, sont les bienvenus.

Canadian Acoustics is published four times a year - in March, June, September and December. This quarterly journal is free to individual members of the Canadian Acoustical Association (CAA) and institutional subscribers. **Canadian Acoustics** publishes refereed articles and news items on all aspects of acoustics and vibration. It also includes information on research, reviews, news, employment, new products, activities, discussions, etc. Papers reporting new results and applications, as well as review or tutorial papers and shorter research notes are welcomed, in English or in French. The Canadian Acoustical Association selected **Paypal** as its **preferred system** for the online payment of your subscription fees. Paypal supports a wide range of payment methods (Visa, Mastercard, Amex, Bank account, etc.) and does not requires you to have already an account with them. If you still want to proceed with a manual payment of your subscription fee, please Membership form and send it to the Executive Secretary of the Association (see address above). - - Dr. Roberto Racca - Canadian Acoustical Association/Association Canadienne d'Acoustique c/o JASCO Applied Sciences 2305–4464 Markham Street Victoria, BC V8Z 7X8 - - secretary@caa-aca.ca

Acoustique canadienne est publié quantre fois par an, en mars, juin, septembre et décembre. Cette revue trimestrielle est envoyée gratuitement aux membres individuels de l'Association canadienne d'acoustique (ACA) et aux abonnés institutionnels. L'**Acoustique canadienne** publie des articles arbitrés et des rubriques sur tous les aspects de l'acoustique et des vibrations. Ceci comprend la recherche, les recensions des travaux, les nouvelles, les offres d'emploi, les nouveaux produits, les activités, etc. Les articles concernant les résultats inédits ou les applications de l'acoustique ainsi que les articles de synthèse, les tutoriels et les exposées techniques, en français ou en anglais, sont les bienvenus. L'Association canadienne d'acoustique a sélectionné **Paypal** comme solution pratique pour le paiement en ligne de vos frais d'abonnement. Paypal prend en charge un large éventail de méthodes de paiement (Visa, Mastercard, Amex, compte bancaire, etc) et ne nécessite pas que vous ayez déjà un compte avec eux. Si vous désirez procéder à un paiement par chèque de votre abonnement, merci de remplir le formulaire d'inscription et de l'envoyer au secrétaire exécutif de l'association (voir adresse ci-dessus). - - Dr. Roberto Racca - Canadian Acoustical Association/Association Canadienne d'Acoustique c/o JASCO Applied Sciences 2305–4464 Markham Street Victoria, BC V8Z 7X8 - - secretary@caa-aca.ca

Contents - Table des matières

Editor's note: A new music is in the air
Éditorial : Une nouvelle musique est dans l'air

A new music is in the air

Dear reader, I am writing you this editorial, with the heart full of joy as we have been able to meet all together again for our Acoustics Week in Canada 2022.

Now, this may sound a bit strange as this June issue is online after the third issue of this year (which was dedicated to AWC 2022). It was a strange year, as we changed the printing company, and this has created some delays in delivering our journal to you. Too many things changed since the pandemic and our old printing company had to be replaced which created some delays, for which I fully apologize.

We have a new layout, much nicer printing quality and more important we will keep our standard of over 200+ mailed copies of CAA as we have been doing for the last 40 years.

Now, it is my great pleasure to present you, our issue. This is fully dedicated to aeroacoustics and engineering acoustics. A first article is about sonic boom and it is written by our great member Joana Rocha and her students at Carlton University.

Then studies about sound transmission across junctions of walls and floors are reported. These studies built our strong attention to international authors, in this case from Brazil, who are targeting our journal for their findings.

We will soon meet again for our fourth issue which will arrive to you in the first weeks of January 2023.

Meanwhile, I wish you a pleasant read.

Umberto Berardi
Editor in Chief.

Une nouvelle musique est dans l'air

Chère lectrice, cher lecteur, je vous écris cet éditorial, le cœur empli de joie, car nous avons pu nous retrouver tous ensemble pour notre semaine canadienne de l'acoustique 2022.

Cela peut sembler un peu étrange, car ce numéro de juin est en ligne après le troisième numéro de cette année (qui était consacré à l'AWC 2022). En effet,ce fut une année étrange : nous avons changé d'imprimerie et cela a entraîné des retards dans la livraison de notre journal. Beaucoup de choses ont changé depuis la pandémie et notre ancienne imprimerie a dû être remplacée, ce qui a entrainé des retards, pour lesquels je m'excuse pleinement.

Nous avons donc une nouvelle mise en page, une meilleure qualité d'impression et, plus important encore, nous conserverons notre quota de 200 exemplaires du JCAA postés à chaque nouveau numéro, comme nous le faisons depuis 40 ans.

Maintenant, j'ai le grand plaisir de vous présenter notre numéro. Celui-ci est entièrement dédié à l'aéroacoustique et à l'ingénierie acoustique. Un premier article parle du bang sonore et il est écrit par notre éminente membre Joana Rocha et ses étudiants de l'Université Carlton.

Ensuite, des études sur la transmission du son à travers les jonctions des murs et des sols sont présentées. Ces études ont attiré notre attention sur les auteurs internationaux, dans ce cas du Brésil, qui ciblent notre revue pour leurs découvertes.

Nous nous retrouverons bientôt pour notre quatrième numéro qui vous parviendra dans les premières semaines de janvier 2023. En attendant, je vous souhaite une agréable lecture.

Umberto Berardi
Rédacteur en chef

Sensitivity Study of Sonic Boom Ground Signature Using Different Axial Distance Step Sizes For Evaluating Near-Field Overpressure

Jacques Gerard Tamayo *[1] **and Joana Rocha** †[1]
[1]Carleton University, Department of Mechanical and Aerospace Engineering

Abstract

To study the feasibility of supersonic commercial airliners, it is essential to better understand the impact of sonic boom caused by the aircraft. For simplicity, a general supersonic airliner concept by Sun et al. was used to conduct this analysis. Using an aircraft model created using Autodesk's Fusion 360 CAD program, the effects of the aircraft volume and lift in the near-field of the aircraft was determined using a custom MATLAB script developed in-house. The near-field overpressure was then propagated using NASA's PC Boom program to determine the ground signature of the airliner. Furthermore, a sensitivity analysis for the geometric and lift properties was conducted. It was determined that an axial step size of 1.2 m (i.e., the spacing between cross-sectional areas obtained from the 3D model used for the numerical differentiation) yields the best results for creating the full ground signature propagated by PC Boom, and that using this step size also results in better computation times compared to smaller step sizes. It was also observed that smaller step sizes for analysis caused noisier/unfiltered data in the F-Function curve which did not change the accuracy of the overall ground signature propagated by PC Boom. Finally, it was determined that a sufficiently large step-size causes the signature propagated by PC Boom to form a different shape compared to step-sizes less than 1.2 m, which should not be considered.

Keywords: Sonic boom, supersonic aircraft, sensitivity analysis

Résumé

Pour étudier la faisabilité d'avions commerciaux supersoniques, il est essentiel de mieux comprendre l'impact du bang sonique causé par l'avion. Afin de simplifier le problème, un concept général d'avion de ligne supersonique, proposé par Sun et al., a été utilisé pour mener cette analyse. Le modèle d'avion a été créé à l'aide du programme de CAO Fusion 360 d'Autodesk, les effets du volume et de la portance de l'avion dans le champ proche de l'avion ont été déterminés à partir d'un script MATLAB développé par les auteurs. La surpression en champ proche a ensuite été propagée à l'aide du programme ≪ PC Boom ≫ de la NASA pour déterminer la signature au sol de l'avion de ligne. De plus, une analyse de sensibilité pour les propriétés géométriques et de portance a été réalisé. Il a été déterminé qu'une taille de pas axial (c'est-à-dire l'espacement entre les sections transversales obtenues à partir du modèle 3D utilisé pour la différenciation numérique) de 1.2 m donne les meilleurs résultats pour créer la signature de sol complète propagée par PC Boom, et qu'en utilisant cette taille on obtient également de meilleurs temps de calcul, en comparaison à des tailles de pas axial plus petites. En outre, il a été observé que pour cette analyse, l'utilisation de tailles de inférieur à 1,2 m produisait des données plus bruyantes/non filtrées dans la courbe de fonction F, ce qui ne modifiait pas la précision de la signature globale du sol propagée par PC Boom. Enfin, il a été déterminé qu'une taille de pas suffisamment grande amène la signature propagée par PC Boom à former une forme différente par rapport aux tailles de pas inférieures à 1.2m, ce qui ne doit pas être pris en compte.

Mots clefs: Bang sonique, avions supersoniques, analyse de sensibilité

1 Introduction

Breaking the sound barrier by travelling faster than the local speed of sound will cause a sonic boom phenomenon, which typically results on a loud boom that can be heard from miles away. The sonic boom phenomenon cannot be avoided for aircraft travelling faster than the local speed of sound and the only way to mitigate the impact of the boom is to minimize the sonic boom which is caused by the aircraft. The sonic boom phenomenon is still a major challenge for modern day engineers designing supersonic aircraft designed to deliver passengers over long distances, in a shorter period of time compared to modern day commercial aircraft.

Minimizing the sonic boom produced by an aircraft were previously researched. For example, the X59 demonstrator aircraft by NASA and Lockheed Martin aims to produce a sonic boom loudness of 75 perceived level loudness (PLdB) at ground level which is equivalent to hearing a car door slam across a street [1]. Mathias Wintzer et al. have conducted a shape optimization process of a conceptual low-boom demonstrator aircraft and achieved an almost 10 PLdB reduction in the sonic boom loudness from the baseline [2]. Scarselli et al. have applied Carlson's method for simplified calculation of sonic boom signatures and conducted an optimization for minimizing sonic boom in their research [3]. Further

∗. jacquestamayo@cmail.carleton.ca
†. Joana.Rocha@carleton.ca

design optimizations for aircraft minimizing the sonic boom loudness were conducted by Rallabhandi et al. where adjoint-based shape optimization to design new low-boom concept models [4]. For the feasibility of supersonic flights, Sun et al. have performed an overview for different supersonic business jet concepts (SSBJ) highlighting the potential issues in environment, aircraft design, sonic boom loudness and ground footprint, aerodynamic efficiencies, and more [5].

The aim of the current study is to investigate the sonic boom phenomenon using a recreated supersonic airliner concept model (SSA) by Sun et al. [6], using a CAD program along with the concept model for sensitivity studies to determine the optimized parameters that should be used for further investigating the sonic boom ground signature of the concept model. Results from this study will allow future work for design optimization and considerations for minimizing the sonic boom ground signature.

2 Method

2.1 Linearized Flow Pressure Field

To study how sonic boom propagates from a vehicle travelling at supersonic speeds, the linearized flow pressure field of the vehicle evaluated at the near-field is required. The linearized flow pressure field of a supersonic vehicle can be determined using the following equation [7] :

$$\delta p\left(\tau;\theta\right)=\frac{\gamma p_0 M^2}{\left(2\beta r\right)^{\frac{1}{2}}}F\left(\tau;\theta\right) \tag{1}$$

The linearized flow pressure field of a vehicle is proportional to the specific heat of air γ, the ambient pressure at the flight altitude p_o, the square of the Mach number of the vehicle M and the *F-Function* of the aircraft F while being inversely proportional to the square-root of two times $\beta=\sqrt{M^2-1}$ and the radial position r evaluated from the centre of the aircraft. The linearized flow pressure field is evaluated at $\tau=x-\beta r$, which is the equivalent axial position of the aircraft translated to a point on the Mach plane formed by the vehicle [6]. The parameter θ is the azimuth angle evaluated at the vehicle coordinate system [7]. The near-field over-pressure, or $\frac{\delta p}{p_0}$, can be determined from equation (2), which is required for PC Boom to propagate the sonic boom of the aircraft at near-field to the far-field to determine the ground signature [7].

2.2 Whittam's F-Function

The *F-Function* depends on both the geometry and lift distribution of the aircraft and is evaluated at axial stations on the vehicle. The *F-Function* was first introduced by Whittam and the concept was extended for wing-body configurations by Walkden [7], being determined using the following equation :

$$F\left(\tau;\theta\right)=\frac{1}{2\pi}\int_0^\tau\frac{A_e''\left(x;\theta\right)}{\sqrt{\tau-x}}dx \tag{2}$$

In equation (2), τ is the axial position of the vehicle translated to a position in the Mach plane, x is the axial position of the aircraft, and $A_e''(x)$ is the geometric second derivative of the equivalent area of the aircraft evaluated at an axial position [6]. Please do note that the area function $A_e''(x)$ is a discrete/numerical function of area data obtained from the 3D model and was not determined analytically with a continuous function using splines or other methods. The equivalent area of an aircraft is defined by equation (4), and consists of two different parts which are the equivalent area due to volume $A_v(x)$ and the equivalent area due to lift $A_l(x)$ [7].

$$A_e\left(x;\theta\right)=A_v\left(x;\theta\right)+A_l\left(x;\theta\right) \tag{3}$$

To calculate the F-Function at any given position τ, axial distance values x were used such that $x>\beta r$ to avoid singularity at $x=\tau$ and undefined integrals at $x<\beta r$.

2.2.1. Equivalent Area Due to Volume

The equivalent area of the aircraft due to volume $A_v(x)$ is the volume of air displaced by the aircraft as it travels through supersonic speeds and is defined as the cross-sectional area of the vehicle cut by the Mach plane tangent to a Mach cone which is projected to a normal axis in a given axial position x [7]. For axisymmetric slender bodies, the $A_v(x)$ is simply the normal cross-sectional area of the aircraft at a given axial distance [7].

2.2.2. Equivalent Area Due to Lift

The equivalent area of the aircraft due to lift $A_l(x)$ is determined using the lift distribution of the aircraft given axial distance and is determined using the following equation [6].

$$A_l\left(x;\theta\right)=\frac{\beta}{2q_\infty}\int_0^x L\left(x;\theta\right)dx \tag{4}$$

Here, $q_\infty=\frac{1}{2}\rho u^2$ is the dynamic pressure of the aircraft at the altitude with ρ as the density of air and u as the airspeed of the vehicle. The integral $\int_0^x L\left(x;\theta\right)dx$ represents the lift cumulative distribution of the aircraft where fully integrating the equation along the axis will give the total lift of the aircraft [7].

2.3 Aircraft Lift Approximation

The approximation of the lift function follows the method outlined by Scarselli et al. to determine the equivalent area displaced by lift required by the F-Function [3].

At level flight, the total lift of the aircraft is equal to the weight of the aircraft at cruising conditions where $L=W=mg$. The general lift equation of an aircraft is defined by [8] :

$$L=\frac{1}{2}C_l\rho u^2 A \tag{5}$$

in which ρ is the density of air, u is the airspeed, A is the total wing planform area, and C_l is the lift coefficient of the aircraft. Using the level flight condition of $L=W$, the lift coefficient of the aircraft can be determined as $C_l = \frac{2W}{\rho u^2 A}$. The lift of the aircraft at a given axial distance $L(x)$ $\left[\frac{N}{m}\right]$ required for the equivalent area due to lift can be determined using the known values of ρ, u, and C_l, as following :

$$L(x) = \frac{1}{2} C_l \rho u^2 b(x) \tag{6}$$

where $b(x)$ is the wingspan of the aircraft at an axial position. The total integral $\int_o^L b(x)dx$, in which L is the aircraft length, is the total planform area of the aircraft wing. Similarly, the total integral $\int_o^L L(x)dx$ is the total lift of the aircraft at level-flight condition.

2.4 Propagating Near-Field Signature to Far-Field

To propagate the near-field overpressure of the aircraft to the far-field for obtaining the sonic boom ground signature, NASA's PC Boom program for Windows (ver. 671) was used. The PC Boom program is a fully ray-traced sonic boom program developed by NASA that can calculate sonic boom footprints and shapes from flight vehicles which can compute various ground signature shapes from different near-field sonic boom signatures [7]. The simple F-Function mode (Mode FFUNC) in PC Boom was used to propagate the calculated near-field overpressure (dP/P) of the SSA model cruising at 55000 ft altitude to determine the ground signature of the SSA model.

2.5 Aircraft Parameters and Design

The aircraft designed for analysis follows the supersonic airliner concept model from a study by Sun et al. as the dimensions are readily available from the study and a 3D model can be recreated using a CAD program for further study [6].

The mass of the aircraft at cruise condition is approximated as 80% of the maximum take-off mass (MTOM). The wing gross area uses the total area obtained by the approximated $b(x)$ function of the aircraft for consistency.

Table 1: Supersonic Airline Concept Model [6]

Aircraft Mass [kg]	78400
Cruise Mass [kg]	62400
Planform Area [m^2]	244.3

2.6 Supersonic Airliner Concept Model Recreation

The supersonic airliner concept model was recreated through AutoCAD's Fusion 360 CAD program using the dimensions from the general geometry sketch of the supersonic airliner concept design by Sun et al. [6], as shown in Figures 1 and 2. One notable difference between the recreated and the general model is the airfoil profile for the wing and elevator. Since it was difficult to determine the airfoil profile used by the general model, an ideal supersonic airfoil using the biconvex model was assumed and used for aircraft wing used to recreated 3D model [9].

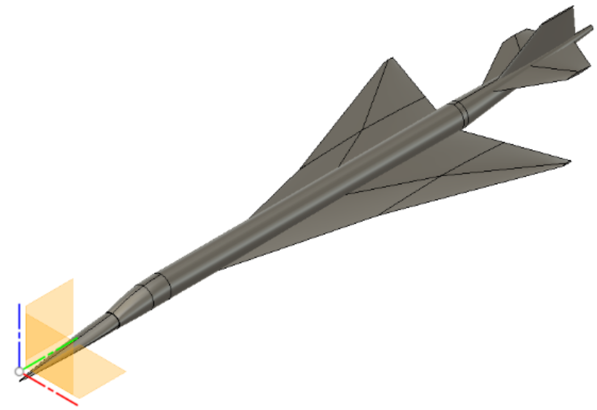

Figure 1: Recreated supersonic airliner (SSA) model in Fusion360 program

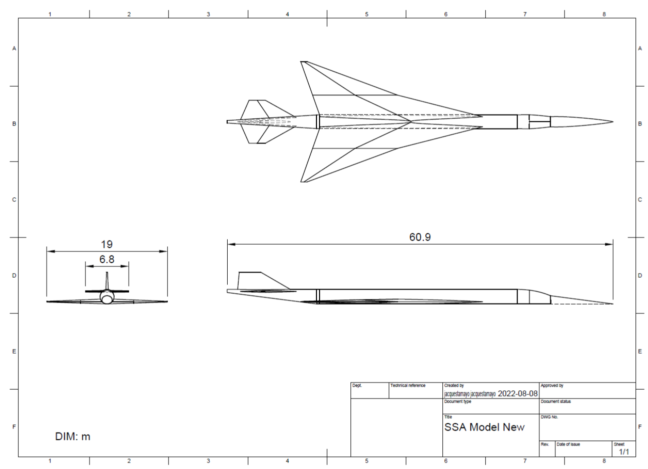

Figure 2: Three-view drawing of the recreated Supersonic Airliner (SSA) Model

2.7 Aircraft Flight Conditions

The aircraft flight conditions will follow the same conditions as the supersonic airliner concept model studied by Sun et al. [6], as shown in Table 2. The testing atmosphere uses the U.S. Standard Atmosphere model for temperature and humidity with no winds blowing at any given altitude. The air density, ambient pressure, and speed of sound at the given altitude were interpolated from charts available in fluid dynamics studies [10].

Table 2: Aircraft Flight Conditions [6]

Altitude (h) [m]	16764 (55000 ft)
Mach Number (M)	1.8
Air Density (ρ) [kg/m^3]	0.157
Air Pressure (p) [N/m^2]	1.371
Speed of Sound (v) [m/s]	295.1

3 Results

As mentioned in previous sections, the 3D model of the supersonic airliner concept was created using Autodesk's Fusion 360 CAD program. Fusion 360 was used to determine the cross-sectional area distribution of the aircraft given axial position. The F-Function and linear flow pressure field was calculated using MATLAB by creating an in-house MATLAB script, which was developed using the equations presented in the methods section. Lastly, the near-field overpressure calculated from MATLAB was used as an input for PC Boom, in order to propagate the sonic boom signature from the near-field to the far-field, to determine the ground signature of the sonic boom. The results for the aircraft geometry, F-Function, near-field overpressure, and propagated ground signature of the sonic boom uses an axial distance step size of 1.2 m for the results section. All step sizes of 0.2 m, 0.4 m, 0.6 m, 1.2 m, and 3.6 m were tested and results for the near-field overpressure, and propagated ground signatures were compiled on one plot for sensitivity analysis, as described in detail in the following sections.

3.1 Aircraft Geometry Functions

This section includes the volume distribution function of the SSA model (Figure 3), the wing geometry used (Figure 4), the area displaced by the lift (Figure 5), and the total area displaced by the SSA due to the volume and lift (Figure 5). The total wingspan of the aircraft is double the wing geometry function shown in the plot to include both sides of the wing.

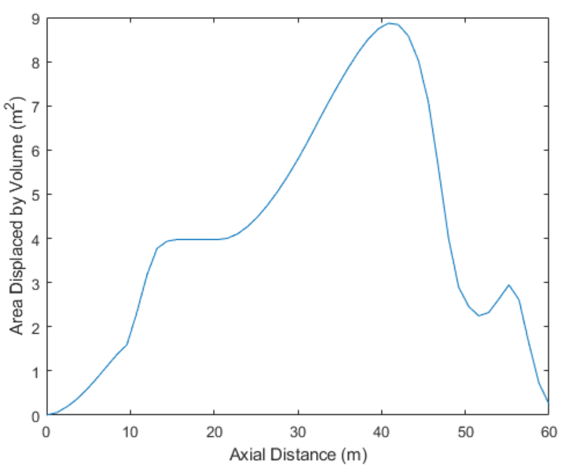

Figure 3: Cross-sectional area distribution of the SSA over axial distance (volume)

The cross-sectional area distribution function from Figure 3 follows the shape of the supersonic aircraft concept where an increase in cross-sectional area can be seen on both the wing section and the tail section, and the cross-sectional area distribution becomes constant after the nose section before the wing. The area displaced by lift uses the wingspan geometry from Figure 4 to form a cumulative distribution function (CDF) where the displaced area peaks at the downstream end of the wing. The total area function displayed on

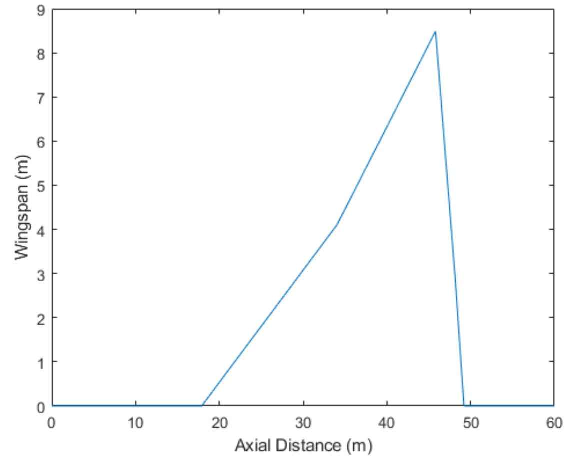

Figure 4: Wing geometry of the recreated SSA model for a single wing

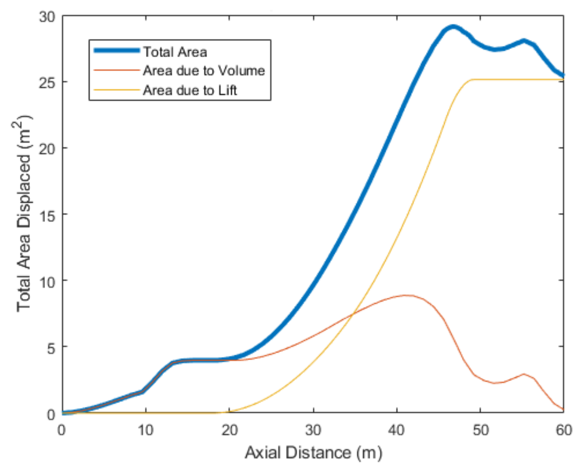

Figure 5: Total area displaced by the SSA due to volume and lift over axial distance

Figure 5 shows that the lift of the aircraft displaces air significantly more than the cross-section or volume of the aircraft and the combination of volume and lift greatly increases the area displaced by the aircraft. The cross-sectional area peaks formed by the wing and tail is more subtle in the total area displaced by the aircraft due to the area displaced by the lift.

3.2 Aircraft Geometry Derivatives

This section includes results for the second derivative functions for the area displaced by volume, the second derivative functions for the area displaced by lift, and the effects of both combined to find the total $A''(x)$ all seen on (Figure 6). Second order numerical differentiation methods, such as second order finite difference methods, were used on the MATLAB script to compute the derivative functions. All step sizes 0.2 m, 0.4 m, 0.6 m, 1.2 m, and 3.6 m were used to numerically differentiate the area functions $A(x)$ obtained from the supersonic airliner model to get the second derivative area functions $A''(x)$.

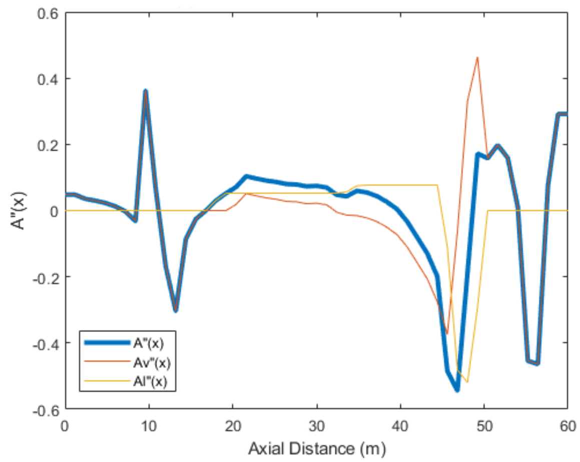

Figure 6: Total second derivative function of the SSA ($A''(x)$) combining area displaced by volume ($Av''(x)$) and lift ($Al''(x)$)

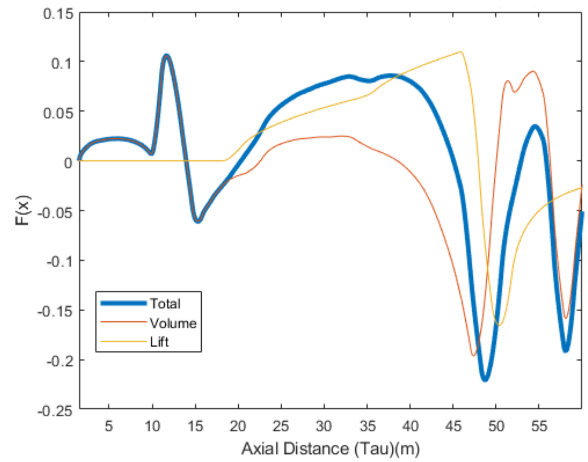

Figure 7: Total F-Function of the SSA model given axial distance compared with volume and lift F-Function

Due to the definition of Whittam's F-Function concerning the requirement of the second derivative of the total area of air displaced by the aircraft, the increase in magnitude of displaced area due to combining the lift contribution to volume is not enough to alter the linearized pressure field produced by the supersonic aircraft. The second derivative area function of air displaced by volume in Figure 6 shows increase in magnitude at places at the middle of the nose cone ($x = 10$ m) and downstream of the wing ($x = 50$ m) followed by a decrease in magnitude. The final increase occurs after the elevators ($x = 55$ m) in the tail. The second derivative area function of air displaced by lift in Figure 6 shows two visible constant lines followed by a sharp decrease downstream of the wing, and zero everywhere without the wing. This is because the wingspan distribution was determined using three different line equations.

Combining the second derivatives of the area displaced by the volume and lift shows that where the second derivative function of volume decreases in the wing section, the second derivative function of lift increases the magnitude in the wing section. This produces a balancing effect seen in Figure 6 where the total second derivative function $A''(x)$ positions itself near the zero magnitude line. One potential method for minimizing the sonic boom of the aircraft is to balance the second derivative of area displaced by volume and lift so the overall second derivative of displaced area have a magnitude that is close to zero.

3.3 F-Function Results

After determining the second derivative functions, one can calculate the F-Function due to the area displaced by both volume and lift (Figure 7). The F-Function due to volume and lift are then combined to find the total F-Function of the recreated SSA concept model (Figure 7). The numerical integration to find the F-Function was done by finding the Riemann sum of interpolated data points of $A''(x)$ with a fixed step size dx of 0.001 m for all test cases with axial step sizes of 0.2 m, 0.4 m, 0.6 m, 1.2 m, and 3.6 m.

The overall shape of the F-Functions for both volume, lift, and total F-Function in Figure 7 is greatly influenced by the shape of the second derivative functions of the area displaced by the aircraft where positive and negative peaks occur in the same places for the F-Function and the second derivative function. Similar to the second derivative function result, the F-Function due to volume and F-Function due to lift can cause a balancing effect in the wing section of the aircraft where a decrease in F-Function due to volume is increased by the increasing F-Function due to lift. It can be seen that total F-Function in Figure 7 decreases downstream of the wing due to the F-Functions due to lift and volume having a negative value, which is also observed for the second order area function. The F-Function due to lift is more effective in balancing the F-Function due to volume at the downstream end of the aircraft compared to the second derivative area function due to the F-Function due to lift having a non-zero and negative value.

3.4 Near-Field Overpressure

This section includes the linearized near-field pressure $\frac{\delta p}{p_0}$ calculated from the linearized flow pressure field equation using the total F-Function combining the volume and lift components, as shown in (Figure 8).

The near-field overpressure on Figure 8 simply follows the shape of the total F-Function of the aircraft with the magnitude being the only notable difference. Therefore, the trend in F-Function must be first examined to conduct a sonic boom minimization process. To minimize the sonic boom ground signature, the F-Functions due to lift and volume must first balance out the magnitude at the wing section and the F-Function due to lift must continuously decrease the F-Function due to volume at the downstream end of the aircraft. This conclusion is also supported by a research article by Sun et al. [6].

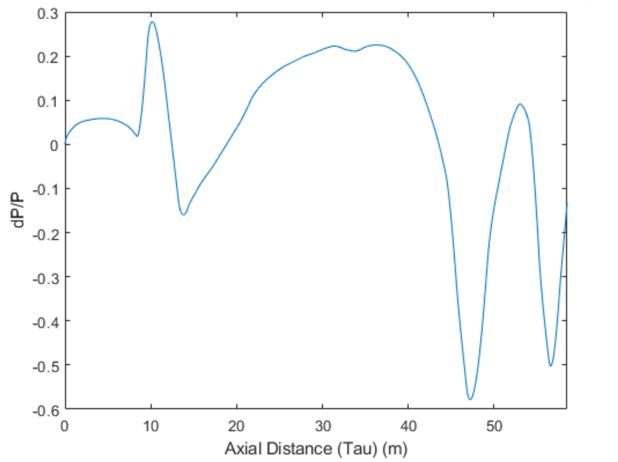

Figure 8: Near-field overpressure $\left(\frac{\delta P}{P_0}\right)$ of the SSA model given axial distance

3.5 Propagated Ground Signature

Once the linearized near-field pressure $\frac{\delta p}{p_0}$ has been calculated, it can be used as an input for PC Boom in order to obtain the propagated ground signature of the sonic boom. Results for the propagated sonic sound signature can be seen in (Figure 9).

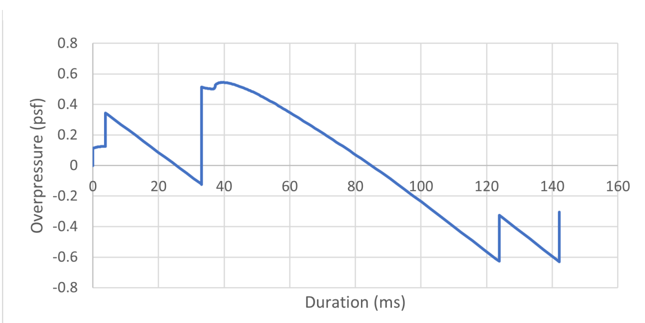

Figure 9: Sonic boom ground signature of the SSA propagated using PC Boom with near-field overpressure input (step size of 1.2 m)

3.6 Near-Field Overpressure (dP/P) Sensitivity Study

The combined results for the near-field overpressure calculated with MATLAB for all the axial step sizes used for sensitivity studies are determined (Figure 10). It is observed that the near-field pressure calculated for smaller step sizes have noisier data in-between and peaks have a higher amplitude for local minima and maxima.

3.7 Ground Signature Sensitivity Study

Finally, the combined results for the sonic boom ground signature propagated using PC Boom from the linearized near-field pressure calculated for all axial step sizes used are determined (Figure 11).

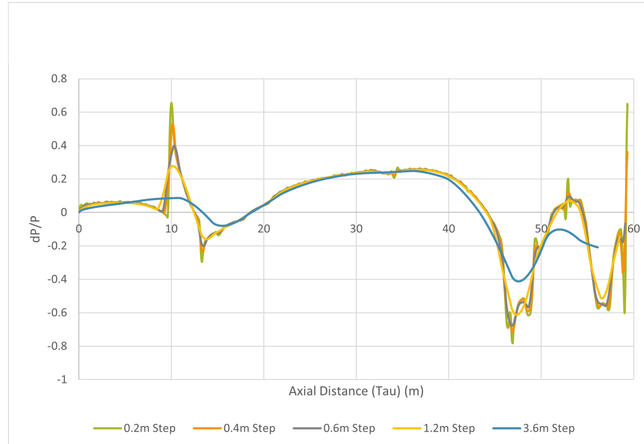

Figure 10: Near-field overpressure $\left(\frac{\delta P}{P_0}\right)$ of the SSA model given axial distance with all step sizes used

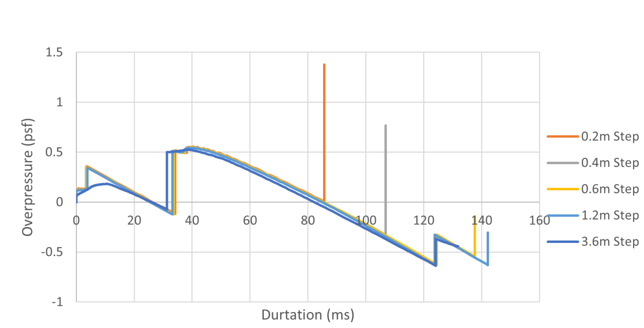

Figure 11: Sonic boom ground signature of the SSA propagated using PC Boom with near-field overpressure input with all step sizes used

3.8 MATLAB Calculation Run Time

The computation time for running the MATLAB script in order to calculate the F-Functions and linearized near-field pressure for the different axial step sizes are relatively inexpensive, as shown in (Figure 12) and Table 3.

Table 3: MATLAB computation time for all F-function and linear flow pressure field calculations with different step sizes

Step (m)	0.2	0.4	0.6	1.2	3.6
Computation (s)	164.28	106.20	86.53	65.68	47.00

4 Discussion

4.1 Near-Field Overpressure and Ground Signature Sensitivity Analysis

Different axial distance step sizes were tested to further understand how it affects the computation of the F-Function and the near-field overpressure of the aircraft. The numerical differentiation to get $A''(x)$ were done using the obtained data points for $A(x)$ and corresponding axial distance x from the Fusion 360 program.

It is observed in Figure 10 that smaller step sizes cause noisier in-between data to form and the peaks can have grea-

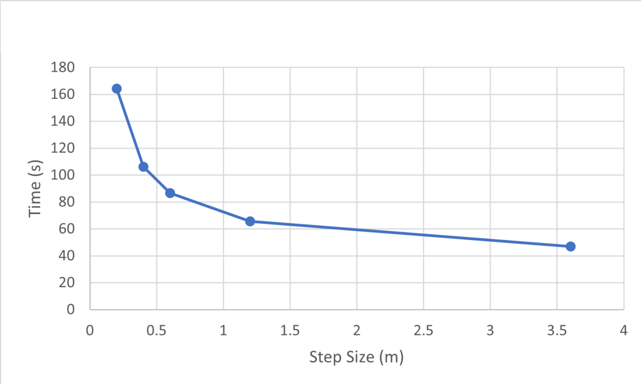

Figure 12: Plotted MATLAB computation time for all step sizes

ter magnitudes as seen at $x = 10$ m. More peaks can be observed for smaller step sizes due to noisier data as a result. It can be seen that the trend of the near-field overpressure for axial distance step sizes of 0.2 m, 0.4 m, 0.6 m, and 1.2 m are consistent in the locations for all the local positive maximum and negative minimum peaks with less noisy/unfiltered data in the near-field overpressure curve in case of the 1.2 m step size. The trend of the near-field overpressure, however, is inconsistent for the extreme case of using a 3.6 m step size where the near-field overpressure trend is only consistent at the wing area of the aircraft between $x = 15$ m to $x = 45$ m. The step size of 3.6 m is sufficiently large enough that the peaks observed in the trend have a much smaller amplitude and is overall inconsistent to the solution.

It is observed that the sonic boom ground signatures for step sizes 0.2 m, 0.4 m, 0.6 m, and 1.2 m have a consistent trend as seen on Figure 11. However, it was determined that PC Boom did not fully produce a complete ground signature for step sizes less than 0.6 m compared to the ground signatures produced using step sizes of 0.6 m and 1.2 m. The step size of 1.2 m shows the full sonic boom ground signature propagated over 142.158 ms while the step size of 0.2 m shows the ground signature ending at 85.692 ms. The step size of 0.6 m showed the second longest signature duration at 137.701 ms while a step size of 0.4 m has the second shortest duration at 106.837 ms. The extreme case of 3.6 m step size showed general consistency with the trend but the sonic boom overpressure shows different trend in the beginning and causes the earliest overpressure compared to other step sizes. The 3.6 m step size case has a sonic boom duration of 131.788 ms which is less than the 1.2 m step size case. Therefore, it is concluded that the step size of 1.2 m should yield the best result for determining the sonic boom ground signature propagated using PC Boom.

4.2 MATLAB Calculation Run Time

A MATLAB computation time analysis was done to further decide the optimal step size for repeat computations. It is observed in Figure 12 that the computation time trend is nonlinear and has diminishing returns for larger step sizes and exponentially longer times for smaller step sizes. Therefore, it can be concluded that the step size of around 1 m (1.2 m tested) is ideal for conducting repeat experiments for saving time in computing the necessary information such as the F-Functions and near-field overpressure using MATLAB.

5 Conclusions

In conclusion, it was determined that the optimal step size for repeat experiments using the MATLAB code and PC Boom for propagating near-field overpressure to producing sonic boom ground signature, is 1.2 m out of the other step sizes used for this test model case (supersonic airliner model). Using a 1.2 m step size will allow short computation times for MATLAB at 65.675 seconds, while producing a near-field overpressure and sonic boom ground signature that is consistent with smaller step sizes with less noisy/unfiltered data which did not change the accuracy and observable trend in the ground signature as propagated by PC Boom for this test case scenario. The shorter computation time and consistent results will allow more repeat experiments to be conducted in order to further study the sonic boom phenomenon.

Future works include testing different geometries for existing or concept aircraft vehicles, and attempting to minimize the sonic boom ground signature by designing an aircraft where the F-Function due to lift and volume can balance both the negative and positive peaks which can theoretically centre the F-Function near the zero-magnitude line.

Acknowledgments

The first author would like to thank Professor Joana Rocha for her supervision and support during the completion of this work.

References

[1] William Jeffrey Doebler and Jonathan Rathsam. How loud is x-59's shaped sonic boom? *Proceedings of Meetings on Acoustics*, 36, 2019.

[2] Mathias Wintzer, Irian Ordaz, and James W. Fenbert. Undertrack cfd-based shape optimization for a low-boom demonstrator concept. *33rd AIAA Applied Aerodynamics Conference*, AIAA 2015-2260, 2015.

[3] Gennaro Scarselli and Francesco Marulo. Sonic boom minimization through a simplified approach for the preliminary design of civil supersonic aircraft. *16th AIAA/CEAS Aeroacoustics Conference*, AIAA 2010-4006, 2010.

[4] Sriram K. Rallabhandi, Eric J. Nielsen, and Boris Diskin. Sonic-boom mitigation through aircraft design and adjoint methodology. *Journal of Aircraft*, 2014.

[5] Yicheng Sun and Howard Smith. Review and prospect of supersonic business jet design. *Elsevier Ltd.*, 2016.

[6] Yicheng Sun and Howard Smith. Conceptual design of sonic boom stealth supersonic transports. *CEAS Aeronautical Journal*, 13 :419–432, 2022.

[7] Juliet A. Page, Kenneth J. Plotkin, and Clif Wilmer. *PCBoom Version 6.6 Technical Reference and User Manual*. 2010.

[8] Daniel P. Raymer. *Aircraft Design : A Conceptual Approach*, volume 6. 2018.

[9] Jacob Siegler, Jie Ren, Leifur Leifsson, Slawomir Koziel, and Adrian Bekasiewicz. Supersonic airfoil shape optimization by variablefidelity models and manifold mapping. *Elsevier Ltd.*, 2016.

[10] Frank M. White. *Fluid Mechanics*, volume 8. 2016.

Comparison of the Sound Transmission Variability with Published Results on Coupling Loss

Max de Castro Magalhaes *[1]
[1]Structural Engineering Department, Universidade Federal de Minas Gerais, Belo Belo Horizonte, Brazil

Résumé

Alors que la plupart des prédictions en matière d'acoustique et de conception des bâtiments utilisent invariablement des modèles publiés et facilement disponibles, une tentative de quantifier les limites de fiabilité qui couvrent la plupart des cas serait très précieuse. Par exemple, il est démontré que certains paramètres (i.e. les dimensions de la pièce, la position des panneaux, l'absorption de la pièce, etc) ont un effet substantiel sur la réduction du bruit et le facteur de perte de couplage, ce dernier étant un facteur très important pour prédire la transmission du son en utilisant l'analyse statistique de l'énergie (SEA). Un modèle SEA a été mis en œuvre et utilisé ici pour la prédiction des facteurs de perte de couplage entre deux pièces. Ainsi, l'objectif principal de cette recherche est d'effectuer une étude paramétrique initiale des facteurs de perte de couplage, puis de comparer leur variabilité avec les courbes théoriques des limites supérieures et inférieures, précédemment présentées dans la littérature pour le couplage des structures. L'utilité de l'EES comme cadre d'analyse peut être évaluée par l'estimation de la variance et des intervalles de confiance. En outre, la moyenne spatiale de la pression acoustique carrée pour chaque sous-système SEA a été estimée via un modèle de synthèse des modes de composantes développé dans un article précédent. En résumé, les pressions acoustiques de la pièce ont été obtenues par une procédure synthèse des modes de composantes et ensuite utilisées dans un modèle SEA où les facteurs de perte de couplage équivalents ont été évalués sur la base des hypothèses SEA. L'influence d'autres paramètres SEA, tels que la densité modale et le chevauchement modal, a également été prise en compte.

Keywords: Transmission du son, analyse statistique de l'énergie, facteur de perte de couplage, étude paramétrique

Abstract

Whilst most predictions in building acoustics and design invariably use published and readily available models, some attempt to quantify confidence limits that cover most cases would be invaluable. For instance, the parameters (e.g. room dimensions, panel position, room absorption, etc.) are shown to have a substantial effect on Noise Reduction (NR) and Coupling Loss Factor (CLF), the latter being a very important factor for predicting sound transmission using Statistical Energy Analysis (SEA). A Statistical Energy Analysis (SEA) model was implemented and used herein for the prediction of CLFs between two rooms. Thus, the main goal this research is to make an initial parametric investigation for the Coupling Loss Factors (CLFs) and then compare their variability with theoretical upper and lower bound curves previously presented in the literature for structure coupling. The usefulness of SEA as a framework of analysis can be assessed by the estimation of variance and confidence intervals. In addition, the spatial-average mean square sound pressure for each SEA subsystem was estimated via a Component Mode Synthesis (CMS) model developed in a previous paper. In summary, the room acoustic pressures were obtained via a CMS procedure and subsequently used in a SEA model where the equivalent CLFs were evaluated on basis of SEA assumptions. The influence of other SEA parameters, such as modal density and modal overlap was also considered.

Keywords: Sound transmission, Statistical Energy Analysis, Coupling Loss Factor, Parametric study

1 Introduction

Although the phenomenon of sound transmission through partitions has been investigated over many years, the problem of low frequency sound insulation in buildings is still an active research area. Modal methods are widely used for the low-frequency analysis of vibro-acoustic problems, including the problem of sound transmission between coupled rooms. On the other hand, Statistical Energy Analysis (SEA) is widely used for mid and high frequency analysis of vibro-acoustic problems. A general introduction to SEA is given in numerous references [1-3] which include discussion on the background theories.

The main advantages of SEA are: it can allow response predictions at mid and high frequencies, where other numerical methods cannot be used; the SEA method involves relatively few degrees of freedom in comparison to other determinist models. The main SEA disadvantages are: the accuracy of predicted average energy is not guaranteed and the model is not capable of modelling local behaviour. Since statistical approaches give statistical answers, they are always subjected to some uncertainties.

The potential errors in the SEA predictions at low frequencies were investigated by Craik *et al* [1, 2]. It was shown that the vibration level difference between two coupled building structures fluctuates with frequency significantly since building structures have few modes at low frequencies.

*maxdcm@gmail.com

The Coupling Loss Factor (CLF) is a statistical quantity defined in terms of the average behaviour of an ensemble of similar subsystems. It relates the power flow between connected subsystems to the stored energy in the transmitting subsystem. It is well-known that significant fluctuations with frequency are observed in the low frequency range. The 'modal overlap factor' is also an important parameter. It is a measure of the degree to which resonant behaviour dominates the response. At low modal overlap, which usually corresponds to low frequency, the actual energy transfer between subsystems can differ considerably from that predicted using the CLF estimates determined from the power transmission efficiencies for semi-infinite subsystems. These fluctuations are in part due to the particular realization of the subsystems within the notional ensemble.

This paper describes an initial parametric investigation into the variability of the effective CLF, in terms of the modal overlap factor and the number of modes in a frequency band. The reliability and accuracy of this empirical model was discussed in comparison with previously published models.

First, the influence of the room dimensions on the CLF has been considered. Numerical experiments were made using sets of simulations, which follow a pre-established analysis pattern. In other words, this analysis was based on the variation of a particular geometrical parameter whilst keeping the others unaltered. Thus, the assessment of the variability and sensitivity of transmission efficiencies to a chosen parameter could be made. In general, there might be some interdependence, but this is outside of the scope of this initial investigation. A total number of 11 iterations were made in order to simulate the original and modified models in each case. The models were obtained by logarithmically varying one dimension at a time (height, width, or depth of receiving room) whilst keeping the others unaltered. For the baseline model, initially a total number of 48, 35 and 97 modes were used for room 1, room 2 and partition respectively. The frequency range and volume sizes considered dictated the choice of the number of modes used. Next, the effects of room absorption on transmission are considered and discussed. Finally, the influence of different panel positions in the common wall between rooms on CLF is considered.

Generally, the sound transmission mechanism in a real building involves a great number of different and complex transmission paths. In SEA these paths are classified as direct and flanking paths [4]. In this study, only the direct transmission was considered in the implemented SEA model, so that the problem was described as one room emitting noise and another room receiving it. The variation of NR with the ratio of the receiving room height to the source room height was considered.

The spatial averaged, time averaged energy for each acoustic subsystem was evaluated from this baseline model, which consisted of two rooms coupled by a limp partition. Later on this paper, one can see that it was necessary to use a limp panel model, so that some parameters (in terms of CLF variability) defined in the literature could be used herein for comparison.

The performance of a building can be predicted by a basic SEA technique, which is described in refs. [1, 2]. The power flow between SEA subsystems can be described by the coupling between them that takes places at their boundaries.

The results that are discussed herein were obtained via simulations using the CMS model developed previously [5]. The analysis was based on considering the influence of some variations in the 'input' parameters, which are required in the pre-processing stage of a numerical experiment, and on the subsequent sound transmission mechanisms of typical building configurations.

Therefore, the main goal of this paper is to examine the variability of CLF to some architectural parameters via a parametric study. This study is aimed at providing not only a better understanding of the sound transmission mechanism in itself but also to produce a useful set of data which for instance can be used by acousticians as input data for a SEA analysis. This data might also be useful for optimizing sound insulation in buildings at low frequencies, where the modal behaviour of rooms strongly influences the transmission. These considerations are discussed in detail in the section 3.

2 The SEA Model

The simplest method of estimating the CLFs is presented here for the sake of simplicity and in order to provide results that can be compared with published data [6]. Although this approach could be used to reduce the computing time required to obtain the CLFs, it is subjected to the common limitations of the Component Mode Synthesis (CMS) method.

The main assumption here is that there are only two subsystems in the SEA model, which correspond to the source and receiving rooms. It seems that this assumed condition is reasonable, as the non-resonant transmission or forced transmission is the most important contribution to the transmission mechanism. In SEA modelling, one of the most important parameters is the modal density. It is defined as the number of modes that lie in an increment of frequency. For instance, the modal density for a standard room is given by [2]

$$n(f) = \frac{4\pi f^2 V}{c_0^3} + \frac{\pi f S'}{2c_0^2} + \frac{L'}{8c_0} \tag{1}$$

where V is the room volume, S' is the total surface area of the room and L' is the total perimeter of the room. Table 1 shows the variation of the modal density for room 2 in the one-third octave band with centre frequency at 250 Hz. The modal density for room 1 was equal to 0.419 in the same frequency band and L_{y1} = 1.8 m. According to Figure 1, the power balance equations for the two coupled rooms (which are represented by the subscripts *1* and *2* and excited one at a time are then given by [3]

$$P_{1,in}^1 = P_{1,diss}^1 + P_{12}^1 = \omega(\eta_1 E_1^1 + \eta_{12}^1 E_1^1 - \eta_{21}^1 E_2^1) \tag{2}$$

$$0 = P_{2,diss}^1 + P_{21}^1 = \omega(\eta_2 E_2^1 + \eta_{21}^1 E_2^1 - \eta_{12}^1 E_1^1) \tag{3}$$

$$P_{2,in}^2 = P_{2,diss}^2 + P_{21}^2 = \omega(\eta_2 E_2^2 + \eta_{21}^2 E_2^2 - \eta_{12}^2 E_1^2) \tag{4}$$

$$0 = P_{1,diss}^2 + P_{12}^2 = \omega(\eta_1 E_2^2 + \eta_{12}^2 E_1^2 - \eta_{21}^2 E_2^2) \tag{5}$$

where η_i is the internal loss factor for each subsystem, E_i is the spatial averaged, time averaged energy in subsystem i.

The CLF from subsystem i to subsystem j is denoted η_{ij}, ω is the angular frequency in radians per second, P_{diss} and P_{in} are the time averaged dissipated and input powers respectively, P_{ij} is the power transmitted from subsystem i to subsystem j. The superscripts 1 and 2 indicate in which subsystem the excitation is applied separately one at a time.

Therefore, by assuming that $\eta_{ij}^1 = \eta_{ij}^2$ and according to the concept of power injection method [2, 3], the 'effective' CLF η_{ij} for two conservatively coupled subsystems 1 and 2 can be obtained by rearranging the equations (3) and (5) as

$$\begin{Bmatrix}\eta_{12}\\ \eta_{21}\end{Bmatrix} = \frac{1}{\omega}\begin{bmatrix}E_1^1 & -E_2^1\\ -E_1^2 & E_2^2\end{bmatrix}^{-1}\begin{Bmatrix}\omega\eta_2 E_2^1\\ \omega\eta_1 E_1^2\end{Bmatrix} \qquad (6)$$

A limp panel model with nominal density equal to 8.1 kg/m^2 was considered. The thickness of the partition was 0.01 m. A Reverberation Time (RT) T_{60}=1 s was considered herein.

For instance, the fraction of maximum stored energy of subsystem 1 transmitted to subsystem 2 per cycle is $2\pi\eta_{12}$, where η_{12} is the CLF. This is defined in the similar way to the definition of the loss factor η of a subsystem, namely $2\pi\eta$ is the fraction of the maximum stored energy which is lost or dissipated per cycle. This can be lost through mechanical and thermal means or can take into account losses due to other subsystems, which have not been explicitly defined.

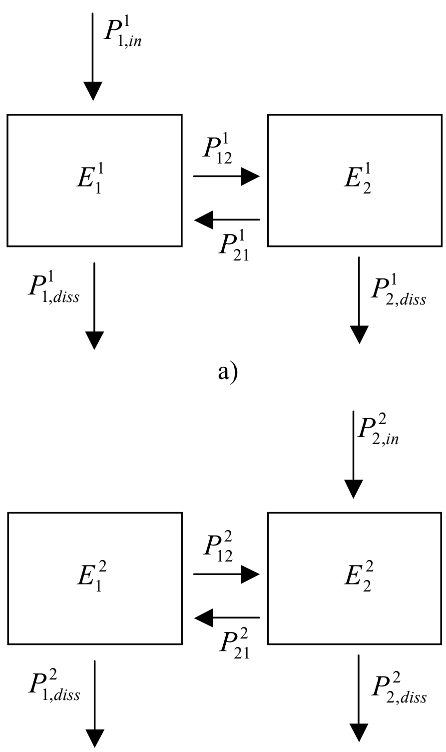

b)

Figure 1: SEA models of two rooms separated by a single-leaf partition approximated by a two-subsystem model. Therefore, only the non-resonant transmission path is considered. a) Power is injected into subsystem 1; b) Power is injected into subsystem 2. The subscripts 'i j' denote the power flow from subsystem 'i' to subsystem 'j' and the superscript indicates which subsystem is under direct excitation.

The spatial average time averaged energy for an acoustic subsystem i can be obtained according to the general expression [1]

$$E_i = \left(\frac{\langle\overline{p_i^2}\rangle V_i}{\rho_0 c_0^2}\right) \qquad (7)$$

where V_i is the volume of subsystem i and $\langle\overline{p_i^2}\rangle V_i$ is the spatial averaged mean square pressure in subsystem $\boldsymbol{i}$. This has been obtained by using the CMS model derived in [1], which was modified to calculate the coupling between the volumes by a limp panel. The calculations were run with no dissipation in the limp panel.

Likewise, the total loss factor of a particular acoustic subsystem i may be approximated by the expression [1]

$$\eta_i = \frac{13.8}{\omega T_{60,i}} \qquad (8)$$

where $T_{60,i}$ is the RT of the subsystem i.

For the SEA simulations $T_{60,i}$ was constant and equal to 1.0 s. Equation (8) is a general expression for the total loss factor which only gives the damping loss factor for weakly coupled systems (i.e. CLFs << internal loss factor) as measurements for the RT will normally include some effect of dissipation from other subsystems connected to the volume. Therefore, a value of $T_{60}$was set and then used to infer the damping loss factor.

Although the CLFs are only defined for finite systems, an expression for the CLF of 'semi-infinite' acoustic subsystems can be obtained by assuming diffuse field conditions in both rooms. In addition, it is assumed that there is direct transmission between rooms, where forced transmission is the most important contribution. Thus, the CLF η_{12} from subsystem 1 to subsystem 2, is given approximately by [1]

$$\eta_{ML} \approx \frac{c_0\, S\, \tau_\infty}{4\,\omega\, V_1} \qquad (9)$$

where τ_∞ is the diffuse transmission efficiency obtained via Mass Law theory described in ref. [5], V_1 is the volume of the source room and S is the partition area.

The CLF η_{21} can also be obtained from η_{12} by the consistency relationship [3]

$$n_1\eta_{12} = n_2\eta_2 \qquad (10)$$

Where n_1 and n_2 are the modal densities (see equation 1) for subsystems 1 and 2 respectively.

The variability of the CLFs with the subsystem properties in SEA models have been recently studied by Park et al [6]. A sensitivity analysis was performed using an analytical model for two coupled plates. The Dynamic Stiffness Method was used in the evaluation of their model. Thus, an 'empirical model' for the variability of CLF (σ^2) was derived for two coupled finite plates according to the expression [6]

$$\sigma^2 = \frac{6}{M_{comb} + N_{comb}^2/16} \qquad (11)$$

where

$$M_{comb} = \frac{2M_1M_2}{M_1+M_2} \qquad (12)$$

$$N_{comb} = \frac{2N_1N_2}{N_1+N_2} \quad (13)$$

where (σ^2 is the variance of the dB values; M_{comb} and N_{comb} are the combined modal overlap factor and number of modes respectively, M_1 and M_3 are the modal overlap factors for subsystems 1 and 2 respectively. They are defined as the ratio of the modal bandwidth to the average frequency spacing between modes [2]. Similarly, N_1 and N_2 are the mode counts for subsystem 1 and 2.

It has been established in ref. [6] that this variance represented a 95.7% confidence interval for all set of data considered for two coupled rectangular plates. Nevertheless, it is not known whether the acoustic system presented herein can be represented by the same value of confidence interval.

3 Results and discussions

Results were obtained in terms of the variation of the CLF ratio with the combined modal overlap factor M_{comb} for different room configurations. The numerical frequency range covered was 0 to 500 Hz, although the results are only plotted at values where at least one non bulk mode exists in either room. Firstly, the CLF ratio, in Figures 2-6, was defined as the ratio of the 'effective' CLF (equation 6), obtained for a particular system configuration, to the averaged 'effective' CLF, which was obtained by considering the mean value over all of the different configurations of a particular parameter, e.g. the height ratio of the rooms. The results were calculated in sets of one-third octave bands. Figures 2-4 show the variation of CLF ratio with M_{comb} whilst varying the height, width and depth ratio of the rooms. In Figure 2, the source room height was fixed and equal to 1.8 m. The receiver height varied from 1.8 to 18 m (see Table 1 below).

Table 1: Variation of room parameters with the height ratio L_{y2}/L_{y1}. L_x, L_y and L_z are room depth, height and width respectively. $n(f)$ is the modal density in the highest 1/3 octave band with centre frequency equal to 250 Hz and f_{Schr} is the *Schroeder* frequency (Hz) above which the acoustic field is assumed to be diffuse. The subscripts 1 and 2 represent the source and receiving rooms respectively.

L_{y2}/L_{y1}	L_{y2}(m)	$n_1(f)$	$n_2(f)$	$f_{1,Schr}$	$f_{2,Schr}$
1.000	1.800	0.419	0.290	430.3	527.0
1.259	2.266	0.419	0.356	430.3	469.7
1.585	2.853	0.419	0.438	430.3	418.6
1.995	3.591	0.419	0.542	430.3	373.1
2.512	4.522	0.419	0.673	430.3	332.5
3.162	5.692	0.419	0.837	430.3	296.4
3.981	7.166	0.419	1.045	430.3	264.1
5.012	9.022	0.419	1.305	430.3	235.4
6.309	11.356	0.419	1.634	430.3	209.8
7.943	14.297	0.419	2.047	430.3	187.0
10.000	18.000	0.419	2.567	430.3	166.6

It is seen that the results lay within the bounds for most of the M_{comb} range. At higher frequencies, the CLF ratio values vary within the range ± 1 dB. Likewise, Figures 3 and 4 also show that the convergence of the results rapidly increases with the combined modal overlap factor.

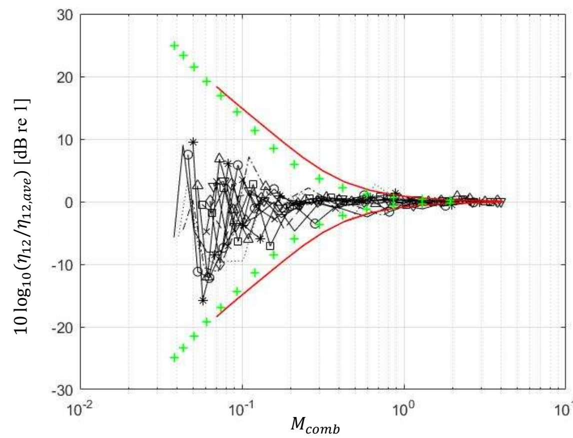

a)

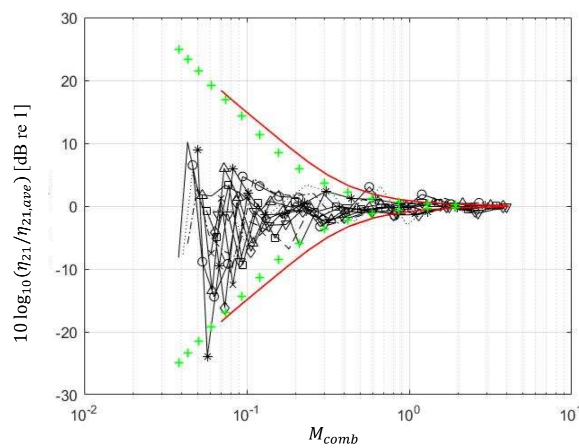

b)

Figure 2: Variation of CLF ratio with the combined modal overlap factor M_{comb} for different values of height ratio (L_{y2}/L_{y1}) compared to the average over all of the height variations.
(a): $10\log_{10}(\eta_{12}/\eta_{12,ave})$ [dB re 1];
(b): $10\log_{10}(\eta_{21}/\eta_{21,ave})$ [dB re 1].
The height of room 1 (L_{y1}) is 1.8 m. The height of room 2 (L_{y2}) varies from 1.8 to 18 m; — 1.8 m; ⋯⋯ 2.27 m; -·- 2.85 m; -o- 3.59 m; -*- 4.52 m; -Δ- 5.69 m; -□- 7.16 m; -x- 9.02 m; -◊- 11.36 m; -∇- 14.29 m; ---- 18 m; +++ bounds ($\pm 2\sigma$) for L_{y2} = 1.8 m; — bounds ($\pm 2\sigma$) for L_{y2} = 18 m.

Figure 3 shows that at higher modal overlap factors, the CLF ratio values tend to be less than ± 0.5 dB. At low frequencies, variability of the effective CLFs is particularly large, while it generally reduces as frequency increases.

However, in Figure 4, the case of varying the depth shows large variation at high frequencies. It might be due to the influence of axially directed modal pattern of pressure that propagates above its cut-off frequency.

Figure 5 shows the variation of CLF ratio with M_{comb} for different values of the RT ratio ($T_{60,2}/T_{60,1}$). The RT of the source room was fixed and equal to 1.0 s. However, for the receiving room it was varied from 1.0 s to 0.2 s. It appears

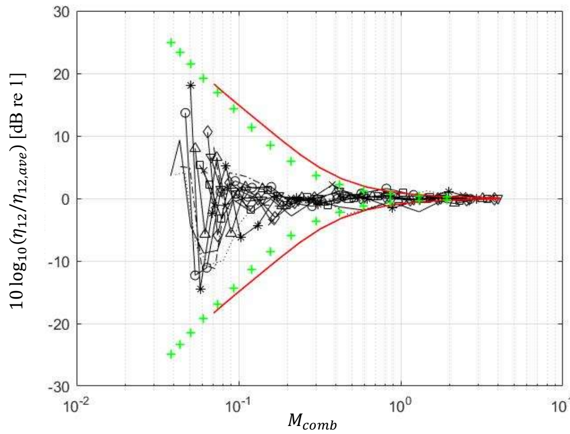

a)

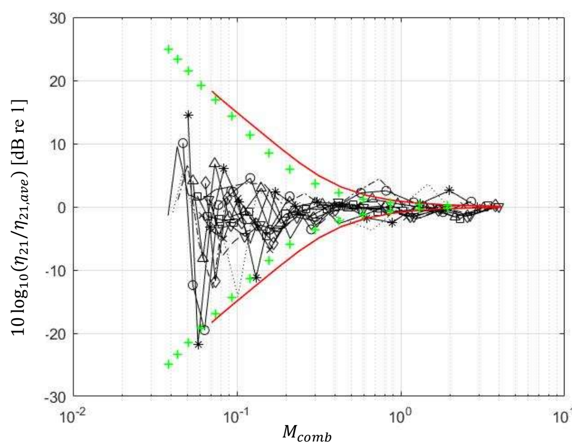

b)

Figure 3: Variation of CLF ratio with combined modal overlap factor M_{comb} for different values of width ratio (L_{z2}/L_{z1}) compared to the average over all of the width variations.
(a): $10\log_{10}(\eta_{12}/\eta_{12,ave})$ [dB re 1];
(b): $10\log_{10}(\eta_{21}/\eta_{21,ave})$ [dB re 1].
The width of room 1 (L_{z1}) is 2 m. The width of the room 2 (L_{z2}) varies from 2 to 20 m; — 2 m; ⋯⋯ 2.52 m; -·- 3.17 m; -o- 3.99 m; -*- 5.02 m; -Δ- 6.32 m; -□- 7.96 m; -x- 10.02 m; -◊- 12.62 m; -∇- 15.89 m; ---- 20 m. +++ bounds ($\pm 2\sigma$) for L_{z2} = 2 m; — bounds ($\pm 2\sigma$) for L_{z2} = 20 m.

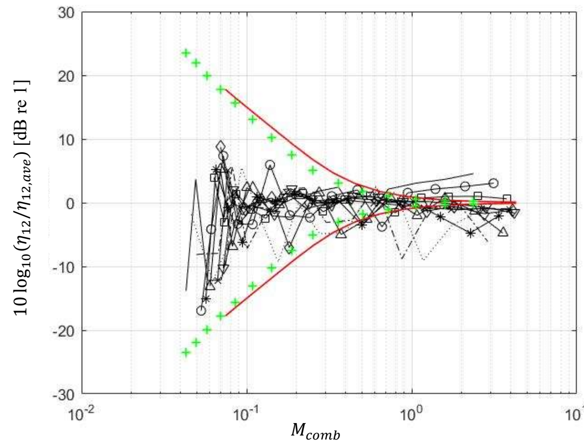

a)

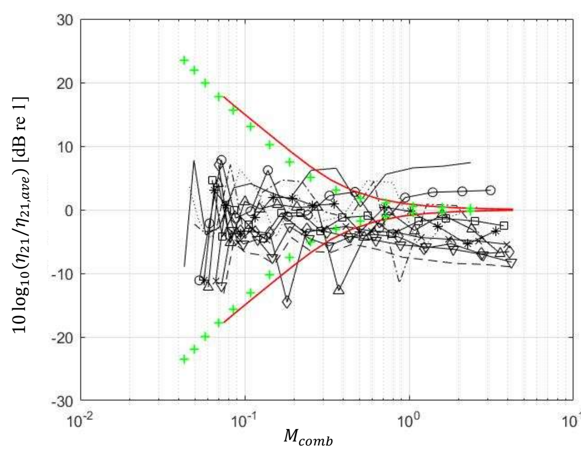

b)

Figure 4: Variation of CLF ratio with the combined modal overlap factor M_{comb} for different values of depth ratio (L_{x2}/L_{x1}) compared to the average over all depth variations.
(a): $10\log_{10}(\eta_{12}/\eta_{12,ave})$ [dB re 1];
(b): $10\log_{10}(\eta_{21}/\eta_{21,ave})$ [dB re 1].
The depth of room 1 (L_{x1}) is 3 m. The depth of the room 2 (L_{x2}) varies from 3 to 30 m; — 3.00 m; ⋯⋯ 3.77 m; -·- 4.76 m; -o- 5.99 m; -*- 7.54 m; -Δ- 9.49 m; -□- 11.94 m; -x- 15.04 m; -◊- 18.93 m; -∇- 23.83 m; ---- 30 m. +++ bounds ($\pm 2\sigma$) for L_{x2} = 3 m; — bounds ($\pm 2\sigma$) for L_{x2} = 30 m.

that the most significant variations in terms of the CLF ratios occurred for the case of varying the RT of the source room whilst keeping the RT of the receiving room constant. As the RT of both rooms increase, the variation in the effective CLF becomes small. At high frequencies (above the Schroeder frequency [5]) when the RT is decreased, the modal overlap factor is increased and vice-versa. This results in a higher probability of better coupling between individual modes and therefore lower sound insulation.

Figure 6 shows the variation of CLF ratio with M_{comb} for different values of panel position on the common rigid wall. Very small variation is observed at the lower values of M_{comb}, i.e. at lower frequencies for the source and receiving rooms where there are few if any acoustic modes and transmission is low. On the other hand, significant variations occur in the range where acoustic modes exist. These variations indicate very high spatial coupling sensitivity. When the frequency increased, oblique modes tended to be dominant in the rooms and the difference between the panel positions became less important on the sound insulation.

The CLF ratio, in Figures 7 and 8, was calculated as the ratio of the 'effective' CLF to the one obtained using equation (9). Although an average result was used for reference, it did not converge to the diffuse incidence Mass Law. It is shown that the variation of CLF ratio, which is defined here as the ratio of the actual transmission to the diffuse incidence Mass Law transmission, with M_{comb} whilst varying the height and width of the receiving rooms.

In Figure 7, the source room height was fixed and equal to 1.8 m. The receiver height varied from 1.8 to 18 m. It is seen that the results approximately lay on the upper bound for

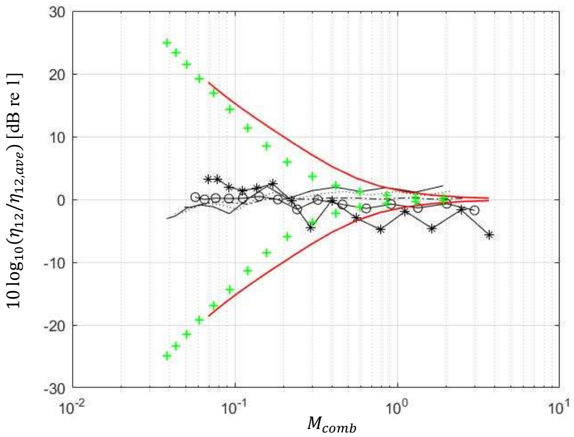

a)

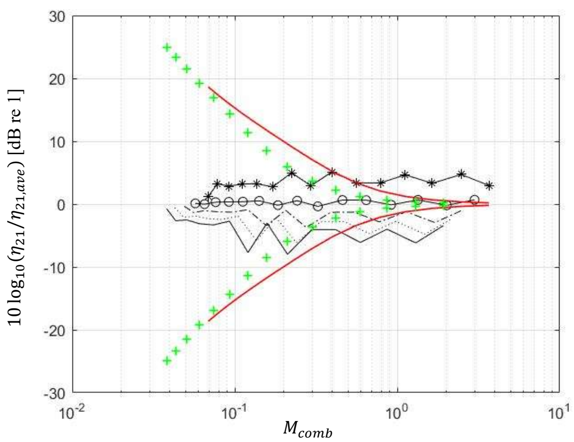

b)

Figure 5: Variation of CLF ratio with the combined modal overlap factor M_{comb} for different values of RT ratio ($T_{60,2}/T_{60,1}$) compared to the average over all of the RT variations
(a): $10\log_{10}(\eta_{12}/\eta_{12,ave})$ [dB re 1];
(b): $10\log_{10}(\eta_{21}/\eta_{21,ave})$ [dB re 1].
The RT of the room 1 ($T_{60,1}$) is 1.0 s. The RT of room 2 ($T_{60,2}$) varies from 1 s to 0.2 s; — 1 s; ⋯⋯ 0.8 s; -·- 0.6 s; -o- 0.4 s; -*- 0.2 s. +++ bounds ($\pm 2\sigma$) for $T_{60,2}$ = 1 s; — bounds ($\pm 2\sigma$) for $T_{60,2}$ = 0.2 s.

most of the M_{comb} range. However, they tend to diverge from the mass law results η_{ML} as the combined modal overlap increases.

Likewise, Figure 8 shows that the mass law results η_{ML} are lower than the 'effective' CLFs at low frequencies. These deviations at high frequencies might be due to effect of resonant modes in the source and receiving rooms included in the CMS model but not in the incident diffuse field mass law assumptions. In other words, this fact was predictable at low frequencies, where the diffuse incidence mass law overestimated the transmission efficiency due to the assumption of diffuse field behavior in the source room. To quantify the reliability of results from the SEA predictions, an investigation on the confidence interval of the coupling between the partition and the acoustic room is also required.

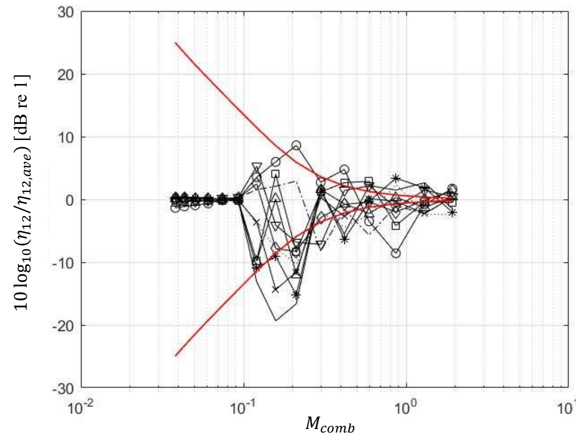

a)

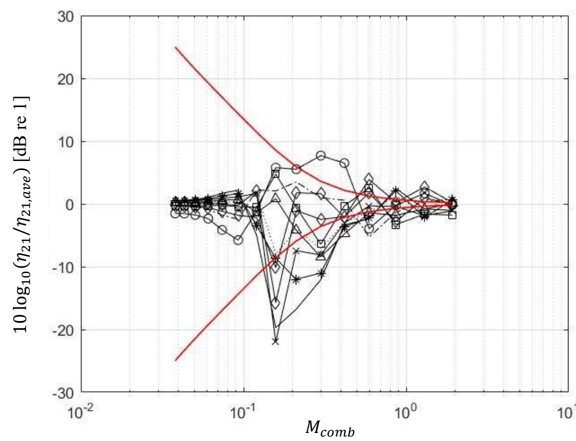

b)

Figure 6: Variation of CLF ratio with the combined modal overlap factor M_{comb} for different values of panel position on the common wall compared to the average over all of the panel positions.
(a): $10\log_{10}(\eta_{12}/\eta_{12,ave})$ [dB re 1];
(b): $10\log_{10}(\eta_{21}/\eta_{21,ave})$ [dB re 1].
— P_1; ⋯⋯ P_2; -·- P_3; -o- P_4; -*- P_5; -Δ- P_6; -□- P_7; -x- P_8; -◊- P_9; -∇- P_{10}. — upper and lower bounds ($\pm 2\sigma$) obtained from equation (11).

There are many uncertainties and potential errors in the low to mid frequency range that still need to be contemplated in the SEA models. At low modal overlap (M< 0.4) the results fluctuate considerably, and most are found to fall within the bounds described herein. The results below the first cut-on frequency of either room were discounted as SEA assumptions would not be valid. For multiple subsystems models the CLFs will not be independent and the SEA prediction requires more detailed investigation.

The 'effective' CLF tends to be lower than the η_{ML} when frequency increases. For a large bandwidth the number of modes in a frequency band is much more important than the modal overlap factor.

In summary, the results obtained shows the variability in the CLF using two coupled acoustic rooms as an example to quantify the uncertainties in the CLF. The CMS was used to quantify the sound pressure response in a wide frequency range. It is seen that a wide range of parameter investigations

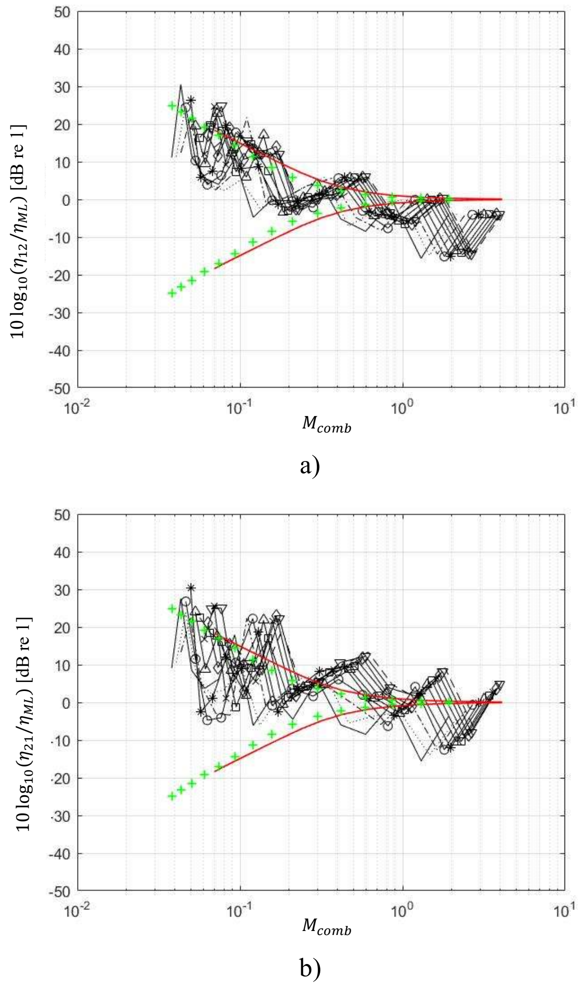

Figure 7: Variation of CLF ratio with the combined modal overlap factor M_{comb} for different values of height ratio (L_{y2}/L_{y1}) compared to the diffuse incidence Mass Law.
(a): $10\log_{10}(\eta_{12}/\eta_{ML})$ [dB re 1];
(b): $10\log_{10}(\eta_{21}/\eta_{ML})$ [dB re 1].
The height of room 1 (L_{y1}) is 1.8 m. The height of room 2 (L_{y2}) varies from 1.8 to 18 m; — 1.80 m; ······ 2.27 m; -·- 2.85 m; -o- 3.59 m; -*- 4.52 m; -Δ- 5.69 m; -□- 7.16 m; -x- 9.02 m; -◊- 11.36 m; -∇- 14.29 m; ---- 18 m; **+++** bounds ($\pm 2\sigma$) for L_{y2} = 1.8 m; — bounds ($\pm 2\sigma$) for L_{y2} = 18 m.

was performed using two acoustics volumes separated by a limp panel. At low modal overlap the CLFs fluctuated with frequency considerably, whereas the variability generally reduced as frequency increased. As the modal overlap factor increases, the bounds of the SEA simulation decrease slightly. It was shown that the SEA predictions are more reliable when the modal overlap factor and frequency bandwidth are large [6], as expected according to the fundamental SEA hypothesis.

4 Conclusion

Numerical simulations for the investigation of the variation of CLF ratio with the combined Modal Overlap Factor were obtained for a limp panel model. Hence, there was no resonance contribution of the panel on the frequency response of

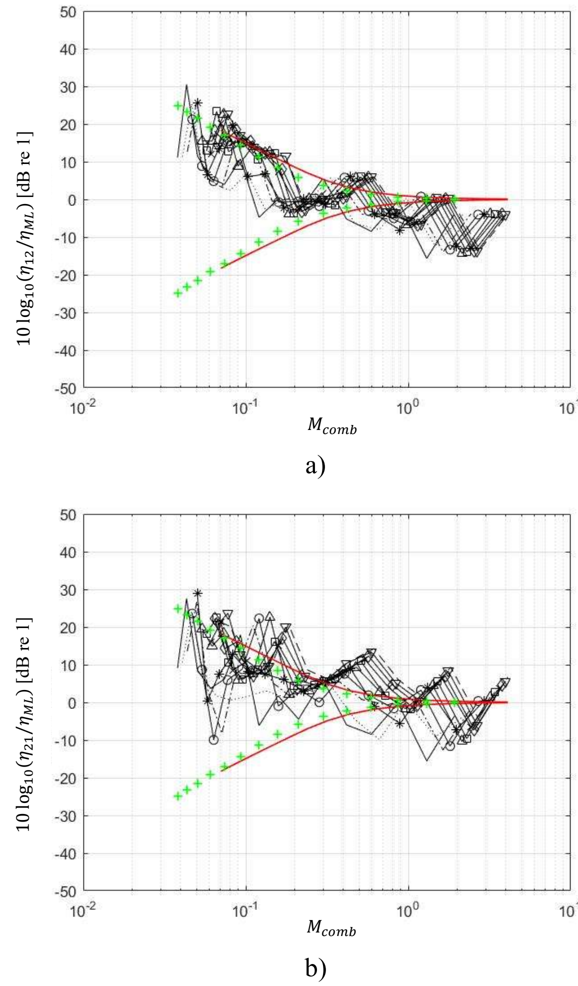

Figure 8: Variation of CLF ratio with combined modal overlap factor M_{comb} for different values of width ratio (L_{z2}/L_{z1}) compared to the diffuse incidence Mass Law.
(a): $10\log_{10}(\eta_{12}/\eta_{ML})$ [dB re 1];
(b): $10\log_{10}(\eta_{21}/\eta_{Ml})$ [dB re 1].
The width of room 1 (L_{z1}) is 2 m. The width of the room 2 (L_{z2}) varies from 2 to 20 m; — 2 m; ······ 2.52 m; -·- 3.17 m; -o- 3.99 m; -*- 5.02 m; -Δ- 6.32 m; -□- 7.96 m; -x- 10.02 m; -◊- 12.62 m; -∇- 15.89 m; ---- 20 m. **+++** bounds ($\pm 2\sigma$) for L_{z2} = 2 m; — bounds ($\pm 2\sigma$) for L_{z2} = 20 m.

the system. Even though there was no stiffness term in the equation of motion of the panel, i.e. the panel was limp, its mass term was allowed to contribute.

The sound transmission results thus had no resonant panel behaviour, and the variation of results were mainly due to the panel position and also the matching or separation of the room natural frequencies (i.e. modal overlap).

The results were then compared to previously published envelope results given for structure-to-structure coupling limits (Park *et al* in reference [6]). It is seen that most of the results, which are presented in terms of CLF ratio, fit reasonably well within the published envelope results [6] for the frequency range investigated. Only the results due to variation of the panel position are not such a good comparison and it is suspected that this might be due to extreme sensitivity of the modal model to the spatial coupling terms. The actual fluid-structure interaction problem considered herein was evaluated at very low frequencies. In addition, small acoustic volumes were considered for the baseline models. Consequently, small values of Modal Overlap Factors were obtained. The envelope results presented by Park *et al* [6] were developed on the basis of only two coupled subsystems, namely two coupled rectangular plates. Hence, there was no 'intermediate' connection between them, such as a beam. In other words, the modal model formulated here was equivalent to the structure-to-structure coupling problem published in ref. [6], as the model herein considered the contribution of a limp partition with no modes on the transmission mechanism.

No attempt has been made here to produce alternative limits for the acoustic-structural problem, as it does not appear to be particular easy to solve or generalize.

Acknowledgments

The author gratefully acknowledges the financial support provided by the Federal University of Minas Gerais (UFMG), the Minas Gerais State Research Foundation (FAPEMIG) and also to the University of Southampton (UK).

References

[1] R. J. M. Craik. The Prediction of Sound Transmission Through Buildings Using Statistical Energy Analysis 1981 *Journal of Sound and Vibration* **82(4),** 505-516.

[2] R. J. M. Craik. Sound Transmission through Buildings using Statistical Energy Analysis. *Gower Publishing Limited*, U.K., 1996

[3] R. H. Lyon and R. G. Dejong. Theory and Application of Statistical Energy Analysis. Boston: Butterworth-Heinemann, Second Edition, 1995.

[4] F.X. Magrans. Definition and Calculation of Transmission Paths Within An S.E.A. Framework. *Journal of Sound and Vibration* 165(2), 277-283. 1992.

[5] M. D. C. Magalhaes. A New Efficient Matrix Algorithm for a 3D Component Mode Synthesis (CMS) Model Used on Sound Transmission Problems. *Computer Modeling in Engineering and Science*, 115 (6), 441-465A, 2015.

[6] W. S. Park, D. J. Thompson and N. S. Ferguson. An Empirical Model for the Variability of the Coupling Loss Factor. *Institute of Sound and Vibration Research – ISVR. Technical Memorandum* 874, 2001.

Vibration Transmission Across Junctions of Walls and Floors in an Apartment Building – A Case Study

Hugo S Libero [*1] and Max de Castro Magalhaes [†1]
[1]Electrical Engineering Department, Universidade Federal de Goiás, Belo Belo Horizonte, Brazil

Résumé

La perception du son rayonné par le sol d'un bâtiment est fortement influencé par les pièces dans lesquelles il est immergé, par les positions de l'auditeur et de la source. La principale question qui reste sans réponse est liée à l'influence de la position de la source sur la puissance sonore rayonnée par un système complexe mur-plancher dans les bâtiments. Cette recherche concerne l'investigation de la transmission des vibrations à travers les murs et les planchers dans les bâtiments. Elle est principalement basée sur la détermination de l'indice de réduction des vibrations par des tests expérimentaux. La connaissance de ce paramètre peut aider à prédire la propagation du bruit et des vibrations dans les éléments de construction. Tout d'abord, les mécanismes physiques impliquant la transmission des vibrations à travers les jonctions structurelles sont décrits. Un montage expérimental est réalisé pour faciliter cette étude. Les tests expérimentaux ont montré que la génération de vibrations dans les murs et les planchers est directement liée à leur taille et aux conditions aux limites. Il est également démontré que la position de la source de vibration peut affecter de manière significative le spectre de vibration global. Ensuite, les caractéristiques des spectres de bruit à l'intérieur des pièces dues à une source d'impact (machine à tarauder) sont également présentées. Des conclusions sont tirées pour la tendance générale du spectre de vibration et de bruit des composants structurels et des pièces respectivement. En résumé, l'objectif de cet article est d'étudier le comportement vibro-acoustique des sols et des murs d'un bâtiment sous l'effet d'une excitation par impact. Les impacts ont été réalisés à des positions distinctes sur la dalle. L'analyse a mis en évidence les principales caractéristiques physiques du mécanisme de transmission des vibrations.

Mots-clés : Transmission des vibrations, indice de réduction des vibrations, excitation par impact

Abstract

The perception of sound radiated from a building floor is greatly influenced by the rooms in which it is immersed and by the position of both listener and source. The main question that remains unanswered is related to the influence of the source position on the sound power radiated by a complex wall-floor system in buildings. This research is concerned with the investigation of vibration transmission across walls and floors in buildings. It is primarily based on the determination of vibration reduction index via experimental tests. Knowledge of this parameter may help in predicting noise and vibration propagation in building components. First, the physical mechanisms involving vibration transmission across structural junctions is described. An experimental set-up is performed to aid this investigation. The experimental tests have showed that the vibration generation in the walls and floors are directed related to their size and boundary conditions. It is also shown that the vibration source position can affect the overall vibration spectrum significantly. Second, the characteristics of the noise spectra inside the rooms due to an impact source (tapping machine) are also presented. Conclusions are drawn for the general trend of vibration and noise spectrum of the structural components and rooms respectively. In summary, the aim of this paper is to investigate the vibro-acoustical behavior of building floors and walls under floor impact excitation. The impact excitation was at distinct positions on the slab. The analysis has highlighted the main physical characteristics of the vibration transmission mechanism.

Keywords: Vibration transmission, Vibration Reduction Index, Impact excitation

1 Introduction

The literature survey has revealed that a significant amount of work has concentrated on analyzing structural response to a dynamic loading using uncoupled structural modes for the building components. In this case the boundary condition at the interface between walls and floors, which is due to the velocity of the corresponding structure, cannot be replicated. Hence, the aim of this paper is to develop alternative 'in-situ' tests for the measurement of vibration transmission. It is performed here initially to structural coupled components to verify the accuracy and applicability of the approach.

Recently, various researchers have concentrated their work on presenting the main advantages of floating floors in terms of their sound isolation effectiveness. The use of floating floors on building construction is well-known among civil engineers, architects, and acoustic space designers. They are popular not only for their ability to decrease the transmission of structure-borne sound throughout the building structural components but also for their slender

[*] hugo.libero@gmail.com
[†] maxdcm@gmail.com

dimension which may be relevant on the calculation of the building total cost price.

Although the physical understanding of floating floor mechanisms is well established, the assessment of the sound power radiated by the structural floor has not been fully considered in terms of its boundary conditions. For example, it is important to know the relationship between the vibration transmission across wall-floor junctions and the sound pressure inside the adjacent rooms. Recently some researchers have concentrated their investigation on optimizing the dynamic models of floating floor systems to improve their effectiveness, i.e., to minimize the transmitted vibrational energy to the structural floor.

The effects of panel boundaries on sound radiation, including a comparison with an infinite panel have been discussed by several researchers [1-3]. A simple two-dimensional model has been used for evaluating the sound radiation characteristics of finite panels [3]. The analysis of the radiation, through a baffled plate of finite width and infinite length was rigorously. The effects of panel size have been studied in frequency regions below, above and at the critical frequency. In addition, estimates of averaged response over a given frequency range have also been investigated. The literature survey has revealed that a significant amount of work has concentrated on analyzing sound radiation of simply supported panels [4-8].

This research was first undertaken as a result of the need to develop an easy and reliable methodology for measuring the floor-wall vibration transmission in order to obtain a better comprehension of the structure-borne vibration transmission across an apartment slab.

2 Experimental tests

The vibration transmission experiments were performed in a particular unreinforced masonry building. The building is composed of four floors. Each structural floor and load bearing wall has a thickness equal to 10cm and 15 cm respectively. The tests were made on the 2nd floor of a particular apartment. The external noise influences were well below the vibration level measurements in the walls and floors, i.e., the signal-to-noise ratio was high enough to assure good quality measurements. The experimental set-up and floor characteristics are shown in Figures 1 and 2 below. First, a tapping machine and accelerometers were positioned on different positions on the floors and walls. The acceleration measurements were made using ICP accelerometers (50 g range, 100 mV/g general purpose accelerometer with 10-32 top connector and 10-32 mounting hole). Before each measurement, the entire arrangement was checked and calibrated.

Next, the total loss factor of each floor and wall was measured indirectly using the structural reverberation time. Impulse responses were obtained using the impact testing procedure described as follows. On impacting the 'panel' by an instrumented hammer, the analyzer was triggered and started recording the response signal at the receiving point, where accelerometers were attached and connected to the acquisition equipment (National Instruments data acquisition module type NI-9234). The input signal was filtered by conveniently configuring the channel parameters. The acceleration levels were obtained via Fourier transforms of the measured quantities.

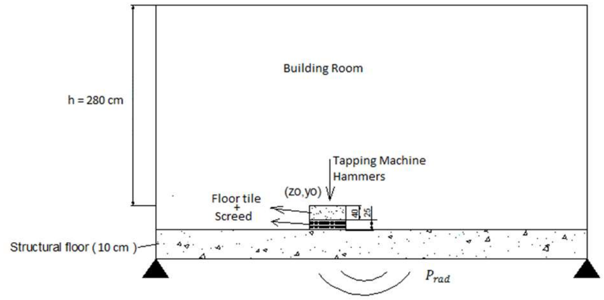

Figure 1: Set-up of the experimental tests.

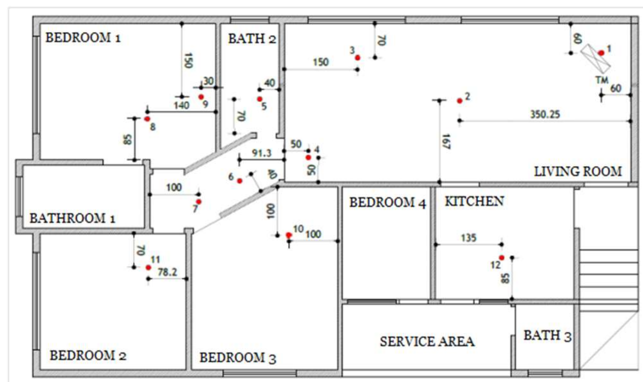

Figure 2: Accelerometer positions on the apartment floor and tapping machine at position TM-1.

A frequency range of 100–4000 Hz was considered on measuring the acceleration levels due to the tapping machine. For the structural reverberation time, decay curves were measured in the frequency range 100-630 Hz, where the signal/noise ratio was high enough and the results were validated. The vibration source was a plastic headed hammer. It was used to hit the concrete panel at different locations (in order to obtain spatial averaged values) over a period of 6 seconds. The velocities were determined by integrating the accelerations at every frequency line

3 Structural Reverberation Time

The structural reverberation time T_s was evaluated from the decay curves from a range of 5 dB to 25 dB below the steady-state level. Within the evaluation range a least-squares fit line was computed for the curve. The slope of the straight line gives the decay rate, d, in decibels per second, from which the structural reverberation time was calculated as $T_s = 60/d$. The commercial software named 'WinMLS' used the impulse responses for the calculation of the reverberation time.

The damping η, known as total loss factor, can be obtained using the following equation

$$\eta = \frac{2.2}{f\, T_s} \qquad (1)$$

where T_s is the structural reverberation time in seconds and f is the frequency in Hertz.

The values of damping η are sometimes termed structural damping, to identify that the damping is dependent on both the damping inherent in the material and that which comes from other mechanisms including dissipation losses at the boundary which might be significant. In other words, the total loss factor is equal to the sum of the internal loss factor of the material, the coupling loss factor to the adjacent structures and the radiation loss factor to the surrounding media [1].

An acquisition time of five seconds was adopted. Figure 3 shows the accelerometer positions on the floors and walls for the reverberation time measurements. At very low frequencies, T_s depends to a large extent on the position of the source and the receiving accelerometer. It is recommended that an ensemble averaging procedure based on a combination of accelerometer positions be adopted for each one-third octave band result.

4 Evaluation of the Vibration Reduction Index $\boldsymbol{K_{ij}}$

In this section the methodology used for the measurement of vibration reduction index $\boldsymbol{K_{ij}}$ of the cross-junction type is described. The vibration reduction index was obtained using the following expression [4]:

$$\boldsymbol{K_{ij}} = \overline{\boldsymbol{D_{v,ij}}} + 10log_{10}\left(\frac{\boldsymbol{L_{ij}}}{\sqrt{\boldsymbol{a_i a_j}}}\right) \tag{2}$$

$$\overline{\boldsymbol{D_{v,ij}}} = \frac{\boldsymbol{D_{v,ij}} - \boldsymbol{D_{v,ji}}}{2} \tag{3}$$

$$a = \frac{2.2\pi^2 S}{c_0 T_s}\sqrt{\frac{f_{ref}}{f}} = \frac{\pi^2 S\eta}{c_0}\sqrt{f_{ref} f} \tag{4}$$

where $\overline{\boldsymbol{D_{v,ij}}}$ is the average vibration level difference between the source element i and the receiving element j (walls, ceiling or floor); $\boldsymbol{L_{ij}}$ is the junction length between the source and the receiver; a is the equivalent absorption length; S is the area; f_{ref} is the reference frequency which is equal to 1,000 Hz; f is the centre frequency; c_0 is the sound phase speed in air and η is the total loss factor.

The vibration source (tapping machine) was placed at particular positions in the building 2nd floor. The corresponding distances between the source and the receivers (accelerometers) are presented in Table 1. The average vibration velocity level was then measured at points shown in Figure 1. The first parameter to be measured was the vibration level in each 'subsystem' (floor and/or wall) which were the source or receiver plate (see Figure 4 below). After that, the structural reverberation time was also measured.

5 Results and discussions

Figure 5 presents the time and space average acceleration levels of the floors. It is seen the variation of floor acceleration levels measured at different points (see Table 1) considering three distinct locations for the tapping machine: living room, bathroom, and bedroom *1*. The values were obtained due to tapping machine generating impact vibrations and the corresponding accelerations being measured at

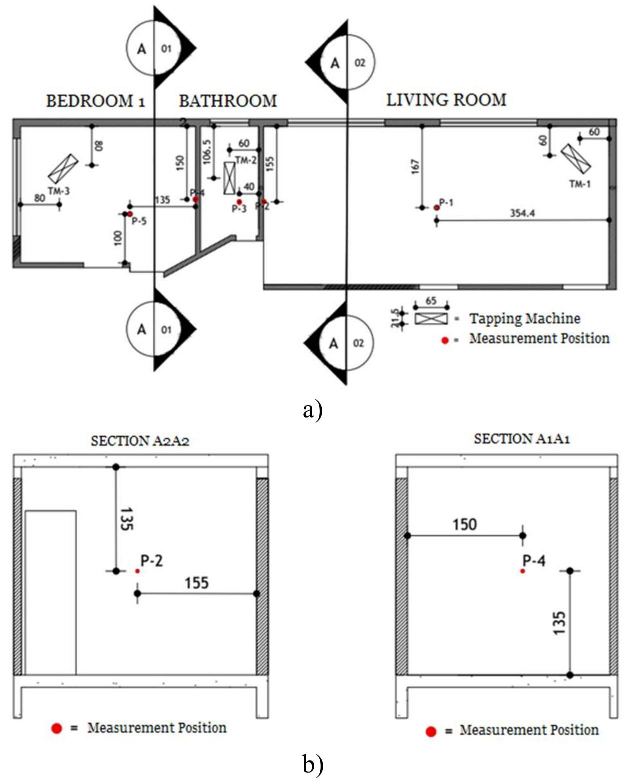

Figure 3: Accelerometer and tapping machine positions on the apartment floor (P-1, P-3 and P-5) and walls (P-2 and P-4). a) Floor plan; b) Floor plan cuts (A_1 and A_2).

Table 1: Distances between the sources (tapping machine at position TM-1, TM-2 and TM-3) and the receivers (accelerometers at positions P-1 – P-5).

Distance Source/Receiver	P-1 cm	P-2 cm	P-3 cm	P-4 cm	P-5 cm
TM-1	313	656	706	795	938
TM-2	430	85	52	82	218
TM-3	780	426	358	288	176

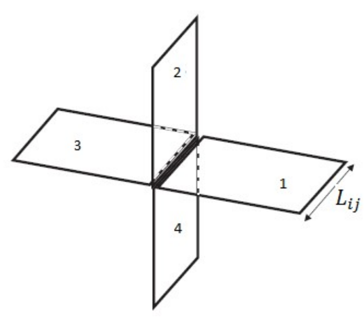

Figure 4: Cross-junction type considered for the determination of the vibration reduction index $\boldsymbol{K_{ij}}$ between floors and walls. The subscripts i, j represent the source and receiver plate respectively.

points P-1, P-3, and P-5 (see Figure 3a). It is seen that the vibration level at point P-5 has the greatest values in the frequency range considered as the tapping machine was on the living room floor (Figure 5a). Likewise, the highest levels of acceleration at points P-3 and P-5 were for the tapping machine located on the bathroom floor and bedroom *1* respectively (see Figures 5b and 5c). It is also observed that the acceleration levels at distinct positions decrease as the distance from the tapping machine increases, as expected.

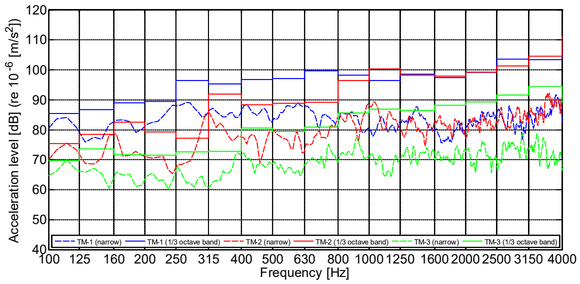

a)

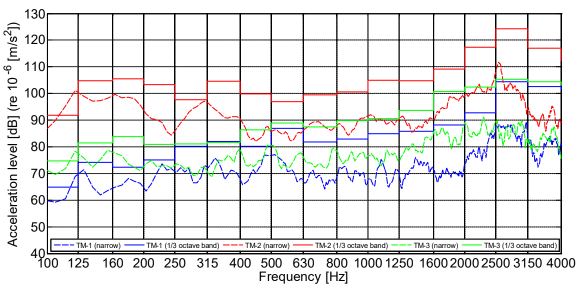

b)

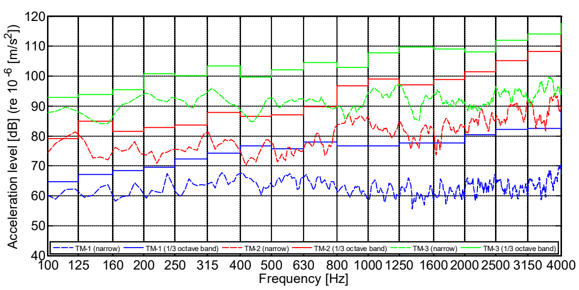

c)

Figure 5: Variation of floor acceleration level measured at distinct points considering the tapping machine location. a) point P-1 (living room ceiling); b) point P-3 (bathroom ceiling); c) point P-5 (bedroom ceiling).

Figure 6 presents the time average acceleration levels of two walls (points P-2 and P-4). It can be observed that the acceleration level varies according to the relative position between source (tapping machine) and receivers (accelerometers), as expected. It is seen that the highest vibration levels are found as the tapping machine was located on the bathroom floor which is supported on two of its edges by the corresponding walls.

In Figure 7 it is seen that the vibrational level is dependent upon frequency and the distance between the source and receiver, as expected. In this case, the tapping machine is fixed at a particular position on the living room floor (see

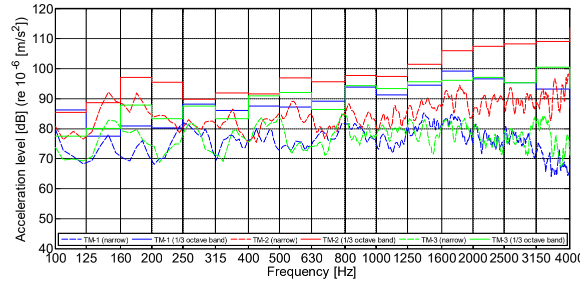

a)

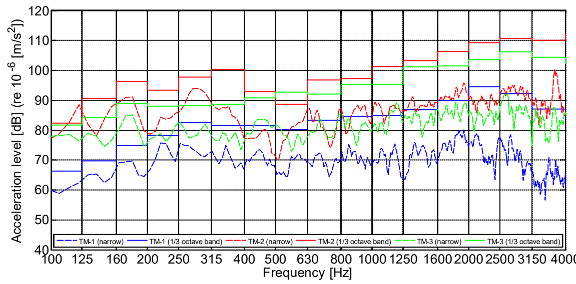

b)

Figure 6: Variation of wall acceleration level measured at distinct points considering the tapping machine location. a) accelerometer on point P-2 (living room wall); b) accelerometer on point P-4 (bedroom wall).

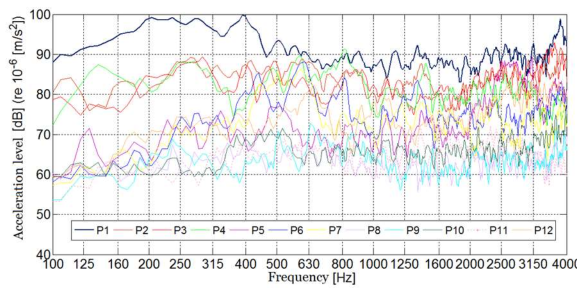

Figure 7: Variation of floor acceleration level measured at distinct positions located in the apartment. The tapping machine location was fixed on the living room floor.

Figure 2). There is a direct correlation between the distance between source-receiver and the acceleration level of the floors in most frequency range. Below 500 Hz, the acceleration levels vary as much as 40 dB. In general, structure-borne vibrational modes are predominant at frequencies below the critical frequencies of the floors. In this case, the critical frequency of the floors was approximately 185 Hz.

Table 3 below shows the acceleration levels in 1/3 octave band centre frequencies (dB re 10^{-6} m/s^2) measured at points P-1 – P-5 illustrated in Figure 3. The level values are presented in the frequency range 100-630 Hz. These values were used in equations (2) and (3) for the determination of the vibration reduction index which are shown in Figure 8.

Figure 8 shows the variation of $\boldsymbol{K_{ij}}$ with frequency. As expected, $\boldsymbol{K_{15}}$ and $\boldsymbol{K_{12}}$ shows the top and bottom values in the whole frequency range. The difference between them reaches 15 dB in the frequency range. On. the other hand, $\boldsymbol{K_{13}}$ and $\boldsymbol{K_{14}}$ present a difference of less than 5 dB between each other.

Table 2: Structural reverberation time of floors (accelerometers at positions P-1, P-3, and P-5) and walls (accelerometers at positions P-2 and P-4).

1/3 octave band (Hz)	T_s(s) P-1	T_s(s) P-2	T_s(s) P-3	T_s(s) P-4	T_s(s) P-5
100	0.53	1.49	0.50	0.46	0.66
125	0.34	0.79	0.41	0.37	0.85
160	0.38	0.38	0.30	0.40	1.28
200	0.33	0.46	0.27	0.27	0.63
250	0.18	0.41	0.15	0.57	0.29
315	0.15	0.28	0.11	0.21	0.15
400	0.21	0.26	0.13	0.16	0.11
500	0.14	0.14	0.10	0.13	0.11
630	0.09	0.14	0.12	0.11	0.10

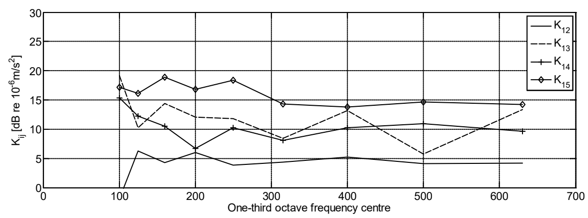

Figure 8: Variation of the Vibration Reduction Index (K_{ij}) with frequency and accelerometer positions P-1 – P-5. Four different situations were considered: $\boldsymbol{K_{12}}$ (TM1 – P-2), K_{13} (TM1 – P-3), K_{14} (TM1 – P-4) and K_{15} (TM1 – P-5).

6 Conclusions

The study presented herein is an alternative for understanding the structure-borne transmission across junctions in dwellings. Flanking transmission via flanked building floors and walls have been investigated using the concept of the parameter named vibration reduction index. This concept is a reliable approach which provides a rapid and practical measurement of the total sound power transmitted into structural panels. The method of measuring vibration acceleration levels, outlined in this study, is a cost-effective technique that can be used in place of traditional techniques which considers the structure sound radiation. In addition, experimental tests can be made in a noisier environment where background noise levels (in one octave band) can be tolerated. The acoustic-based technique may be alternatively applied to mechanical vibration techniques. The influence of vibration level exposure on the physiological and psychological behavior of humans inside residential buildings is already under investigation as part of future work.

Acknowledgments

The author gratefully acknowledges the financial support provided by the Federal University of Minas Gerais (UFMG) and CNPD (National Council for Scientific and Technological Development).

Table 3: Acceleration levels in 1/3 octave band centre frequencies (dB re 10^{-6} m/s^2) measured at points P-1 – P-5 (see Figure 3) as the tapping machine change positions in the apartment rooms (living room, bathroom, and bedroom 1).

Acceleration level [dB re 10^{-6} m/s^2]	**100 Hz**	**125 Hz**	**160 Hz**	**200 Hz**	**250 Hz**	**315 Hz**	**400 Hz**	**500 Hz**	**630 Hz**
AL (TM-1, P-1)	85	86	89	90	96	95	97	97	99
AL (TM-2, P-1)	75	78	83	79	77	92	88	88	89
AL (TM-3, P-1)	69	73	72	72	73	73	81	79	81
AL (TM-1, P-2)	86	77	81	80	88	86	88	87	89
AL (TM-2, P-2)	85	89	97	95	89	92	92	97	96
AL (TM-3, P-2)	78	80	88	8	88	8	91	92	87
AL (TM-1, P-3)	65	74	72	75	80	82	80	87	81
AL (TM-2, P-3)	92	105	106	103	98	105	99	97	99
AL (TM-3, P-3)	75	81	84	81	81	82	86	89	87
AL (TM-1, P-4)	66	69	75	78	83	82	82	80	83
AL (TM-2, P-4)	82	91	96	93	98	100	93	89	96
AL (TM-3, P-4)	82	84	89	88	88	89	91	93	92
AL (TM-1, P-5)	65	67	68	70	72	74	77	76	78
AL (TM-2, P-5)	79	85	82	82	84	88	87	87	90
AL (TM-3, P-5)	93	94	95	101	100	104	99	102	105
Max	93	105.7	105.5	103.2	1002	104.7	99.9	102.2	104.5
Min	64,8	67,2	68.4	69.6	72.4	72.8	76.7	75.7	78.0
Avg	78,5	82,4	85,1	84,8	86,4	88,4	88,7	89,4	90,3
Var	84,9	96,1	114.1	101.9	80.7	93.9	49.3	52.8	59.3
Stdn	9.2	9.8	10.7	10.1	9.0	9.7	7.0	7.3	7.7

References

[1] F. Fahy, *Sound and Structural Vibrations.* Academic Press, London, 1985.

[2] F. G. Leppington, E. G. Broadbent and K. H. Heron, The Acoustic Radiation Efficiency of Rectangular Panel. *Proceedings of the Royal Society of London. Series A, Math. and Physical Sciences,* 1982, 382, 245-271.

[3] M. D. C. Magalhaes and N. S. Ferguson, The development of a Component Mode Synthesis (CMS) model for three-dimensional fluid-structure interaction, *J. Acoust. Soc. Am*. 2005, 118, 3679-3691.

[4] C. Hopkins, C. Crispim, J. Poblet-Puig and C. Guigou-Carter, Regression curves for vibration transmission across junctions of heavyweight walls and floors based on finite element methods and wave theory, *Applied Acoustics*. 2016, 113, 7-21.

[5] Rabold A.; Buschshmid, M.; Duster, A.; Muller, G.; Rank, E. Modelling the excitation force of a standard tapping machine on lightweight floor structures. *Building Acoustics*, 2010, vol 17, num 3, p. 175-197.

[6] Shi, W. Johansson, C., Sundback, U., An investigation of the characteristics of impact sound sources for impact sound insulation measurement. *Applied Acoustics*, 1997, v.51, 85-108.

[7] Shin, K., Park S., Kim, K. Sound prediction based on footstep-induced vibrations in concrete building using a convolutional neural network, *Applied Acoustics,* 2022, v. 198, p. 1-8.

[8] Schiavi, A., Astolfi, A., The prediction of the vibration reduction índex Kij for brick and concrete rigid junctions. *Applied Acoustics* 2010, 71, 523-530.


stravibase
by CDM Stravitec
Building Base Isolation
Structural Vibration Isolation Solutions
CDM Stravitec has been a pioneer in building base insulation projects around the world since the early 1960s. Since then, we have developed several Stravibase structural fixation and building base isolation solutions to mitigate unwanted vibrations and reduce impact and airborne noise.
Stravibase SpringBox
Pre-compressed spring bearings for minimal building deflection
High Load Capacity
Replaceable & Inspectable
Failsafe Mechanism
Buildings near railway or subway lines can be subjected to ground-borne vibrations resulting in structure-borne noise affecting the occupants' comfort within the building.
Structural isolation bearings protect the building and its occupants from these vibrations, making the world a quieter place.
Stravibase Raft
Resilient continuous supporting bearing system
Stravibase VHS
Very high stress elastomeric bearings with added steel plates
Patented Technology
Stravibase SEB
Series of elastomeric bearings laminated to formwork
Discover the full Stravibase product range here.
SCAN ME
TORONTO - LANCASTER - NEW YORK - LOS ANGELES - DALLAS
INFO-CA@CDM-STRAVITEC.COM / INFO-US@CDM-STRAVITEC.COM / WWW.CDM-STRAVITEC.COM

CANADIAN ACOUSTICAL ASSOCIATION

Minutes of the Board of Directors Meeting
Friday, 3 June 2022 13:30 – 16:30 PM (EDT)
by Zoom videoconference

1. Call to Order

Meeting called to order at 13:35 PM (EDT)

Board members present online: Jérémie Voix (chair), Alberto Behar, Umberto Berardi, Victoria Duda, Bill Gastmeier, Bryan Gick, Dalila Giusti, Michael Kiefte, Andy Metelka, Hugues Nélisse, Roberto Racca, Joana Rocha (joined later), Mehrzad Salkhordeh.

Jérémie proposed some rearrangements to the agenda to accommodate other time commitments by members of the Board; he invited the Treasurer to present first, followed by the awards coordinator.

2. Treasurer's Report (Dalila Giusti)

Dalila indicated that revenues are in good shape and there is not much to report regarding the financial picture. Fiscal year end accounting is being readied for 30 June and financial statements will be presented at the Fall meeting.

Investments in the Association's capital fund are doing well; interest rates are increasing and thus driving up the yield of GIC's. Given the good financial picture Dalila suggested that the Board consider an increase in the cash value of the awards (to be discussed at the Fall meeting). She noted that the operating fund has ample balance to cover the expenditures and does not generate much revenue in a bank account, but it would be imprudent to shift money into the capital fund as that is a one-way flow and could lead to a shortfall in meeting unexpected demands. She proposed instead to invest $50k of the operating fund into a 3-year GIC not tied to the capital fund, and also invest $50k of available cash balance in the capital fund into a 5-year GIC to benefit from rising interest rates. After discussion the Board approved the proposal.

In other matters, Dalila noted that the cash prize value of the Audience Award for Best Presentation at the virtual 2021 AWC event had never been explicitly agreed but should have been in the order of $500. This was confirmed by Jérémie and Dalila indicated that she would send the prize to the winner without further ado (she noted that all cash prizes are now delivered by e-transfer). Lastly, she informed the Board that the $2000 seed capital for the 2022 in-person AWC in St John's, Nfld had been deposited in the bank account set up for the event and was available to the organizers.

3. Awards Report (Victoria Duda)

Deadline to nominate candidates for 2022 awards has been extended to end of June; several nominations have been received but still some prizes have no candidates. A winner for the Canada Wide Science Fair award (externally judged) had not yet been announced.

Victoria noted that she has been familiarizing herself with the role of Award Coordinator she took over from Johana Rocha, but she still needs to pick up the threads on processes like the adjudication of the Directors' Award which recognizes each year one student paper and one regular paper published in Canadian Acoustics. Jérémie remarked that there had already been a hiatus of a couple of years in the granting of that prize because of the complexity of arranging the group ranking by the Directors; Hugues offered to assist Victoria in rekindling the process as he had been involved previously in its management.

Dalila commented that the low turnout of applications may be related to lack of motivation on the part of potential applicants because of the modest dollar amount of the cash prizes; sha suggested that greater traction might be achieved if the prizes were $750 instead of $500. In the comprehensive discussion that followed there was consensus that more money should be allocated especially given the economic difficulties faced by students especially at the present time, but better promotion of the awards as well as public acknowledgement of the winners and their institutes is also essential. Jérémie proposed that a revamped awards package be presented at the AGM during the next, in-person Acoustics Week in Canada conference in the autumn.

4. President's Report (Jérémie Voix)

Jérémie updated the Board on the situation with the online Journal and membership management site (OJS), which has been experiencing difficulties since the host OpenJournalSystems.com performed an unannounced version upgrade which broke many of the automation and querying functionality (including e-mail notifications of renewals etc.). This also created substantial obstacles to the Journal production and even led to Google dropping the full-text indexing of the journal archives. Much time and effort were spent by Jérémie and his team on addressing the problems with the hosted site.

Jérémie briefly touched on the several development projects that he had proposed at the 2021 Spring meeting of the BoD for tasks ranging from the revamping of the Association's main web site to the creation and updating of manuals and procedure guides, to improved language support for the Canadian Acoustics subscription and membership management site and more. Sporadic progress has been made on some of those projects by Board volunteers who have taken up various tasks, but Jérémie noted that he had not been able to dedicate much effort to their oversight due to his commitment to some other crucial activities.

One such activity that has been successfully completed by Jérémie and his associate Cécile Le Cocq is the rollout in the Journal management portal of a new type of "subscription" for advertisers, with yearly duration (4 issues) and varying costs reflecting the size (full, half or quarter page) of the desired insertion. This subscription-like paradigm simplifies the ad placement process and its renewal, provides reliable payment online, and gives advertisers access to the current issues of the journal in which their insertion is run. All the programming associated with this development was carried out by Cécile within the Board approved budget of $700. As the process neared completion, however, ongoing problems with host openjournalsystems.com resulted in loss of functionality and waste of resources.

This, Jérémie explained, prompted the decision to repatriate the hosting of the journal and membership management site back to a local server on CWH. While inexpensive and fully under direct control, however, this solution has required a large amount of manual intervention on Jérémie's part and is not sustainable in the long term as the host resources are too limited. He proposed therefore to make one more transition to a professionally managed hosting system, but this time use a service by Simon Fraser University specifically tailored to the requirements of the OJS environment, which was developed at SFU. The solution is more expensive than other options but would save considerable time and effort now wasted in maintenance tasks; the required service echelon for our needs would cost USD 2,700 annually – possibly reduced to USD 1,200 if the Association qualifies for institutional pricing as it is likely. The Board expressed strong favour to adopting this solution if it meant a stable, responsive hosting by an organization fully vested in the OJS technology; the proposal was approved. Some members, however, suggested looking at other organizations such as the Australian Acoustical Society (similar in size to the CAA, and likewise running a formal journal) to determine whether their framework for online resources management might be superior to the OJS.

As a last item of new business, Jérémie gave the floor to Alberto who announced that after many years on the Board he will not be seeking re-appointment at the upcoming AGM. Jérémie on everyone's behalf expressed gratitude for Alberto's long service. He also noted that the newly opened position on the Board would enable Victoria to join as a regular member after being appointed to a special adjunct role for one year. On that note he encouraged all Board members to consider both continuity and renewal in making plans for their tenure.

5. Secretary's Report (Roberto Racca)

As per usual practice the presentation began with a tally of memberships at latest count: 144 regular and 22 student members, lower than the 168 regular and 27 student members reported at the October 2021 Board meeting and essentially back to or just below the numbers of one year prior as reported at the Spring 2021 meeting. The number of sustaining subscribers remained essentially steady at about 20, which is a good base of much valued support but points to the need for ongoing outreach to companies. Roberto noted that the increase in the October membership numbers could have been reasonably attributed to people having signed up in the period leading to the 2021 virtual conference, but the subsequent drop in the current numbers cannot be caused by the waning of that surge (since those new members would still be current) and points to other, more established members not having renewed. He pointed out that his ability to keep track of renewal patterns had been curtailed by the system no longer sending him renewal notification e-mails due to ongoing technical problems described earlier by Jérémie, which could also have resulted in members not having received renewal reminders and thus having allowed their memberships to lapse.

The newly introduced category of retired member attracted two persons, and Roberto expressed hope that in time this group would consist not only of current regular members making the transition upon reaching retirement, but also of former members who had left the Association upon retirement now rejoining it at the more affordable rate. He advocated some form of membership drive aimed at reaching this group, in the context of a very much needed overall effort to better promote membership in general. Also new is the paradigm of managing of advertisers as subscribers, which attracted 7 full-page annual (four issues) runs handled fully through the online platform.

In terms of day-to-day activities, Roberto indicated that he kept up providing support to members requiring manual intervention to address difficulties with the online portal and responding to various queries regarding matters of the Association. He noted his intention to work on the improvement of the OJS portal clarity in its bilingual language support, one of the internal initiatives proposed by Jérémie for which he volunteered.

There was some discussion among Board members regarding the decrease in membership numbers and how it could be caused by a wide range of reasons from COVID to e-mail overload (the idea of offering the choice of text reminders was suggested, as was an auto-renew option), but the dominant message was that a greater degree of personal and targeted engagement of potential new members from among one's professional contacts and networks would have a greater success than any broad online campaign.

6. Upcoming Meetings - AWC 2022: St. John's (Len Zedel)

[Guest; joined ~15:00 EDT for this part only]

Len indicated that all is going well with the organizing of the in-person event; he and co-chair Ben Zendel have been splitting duties between themselves and have a strong team of volunteers. He credited the event planner website for ensuring that everything falls into place.

A student volunteer is working on the public website, and Memorial University colleague Lorenzo Moro is reaching out to industry for sponsorships. Jérémie noted that he received that morning from Ben an announcement to be posted to all the CAA social media channels and sent to a substantial distribution list of previous conferences attendees.

Len talked about the rationale for setting the conference pricing (entrance fees), saying that it had been challenging to work out the costs for the various components – catering being a main one – and how to cover them from fees; they looked at past fee structures and created a formula that seemed to suit the expected attendance for the event. They kept the student fees low (about half the regular fees) as per past practices and based the pricing structure on 100-150 attendees, reaching a full-event fee of $650 for CAA members and $800 for non members.

Sponsorship levels were hard to decide since recent previous examples were for larger urban centres in different geographic regions; they converged on $5,000 for gold and $3,000 for silver sponsorship with possibility of smaller levels of commitment. There are substantial uncertainties on which industrial players may attend and support the conference given its unprecedented location and it being the first in-person after the pandemic hiatus.

Submission of abstract has gone live on the site, and hotel registration at the preferred conference rates has been set up on the Sheraton reservation portal. Application for student travel support is documented online, along with information on the student presentation award.

Len noted that the organizing committee and volunteers are from a very diverse spectrum of academic backgrounds. Also, they have been working on a special session on teaching in acoustics and will be bringing in some teachers to participate in a round table discussion (some travel funding has been made available). Still open to include various levels of teaching and topics as long as they are relevant to the school curricula. Board members offered various suggestions for presenters or presentations.

Entertainment for the social events has been arranged, as is a performance of the "harbour symphony" produced by ship's horns in the city harbour. Also, DFO may provide a lecture on acoustic aids to navigation (perhaps a keynote). At the moment Michael Schutz has been lined up as a keynote speaker, and candidates are being contacted for the other two.

7. Editor's report (Umberto Berardi)

The journal has been faced with a double problem, both from the previously mentioned OJS difficulties that hindered the editorial and production process, and more critically from the printing company that produced the journal for the past three decades having gone out of business. A new company was identified, and it printed last year's September issue, then it too went into difficulties and could not print the December issue. So far, a new company has not yet been selected to print the outstanding issues.

The journal production is continuing at least in digital form; Vol. 50 issue 1 is ready to be published digitally this week; issue 2 will be a regular issue and already has a couple of papers accepted (the workflow for interacting with authors is being hindered by OJS issues so a clumsier email based approach is being used), and issue 3 (September) will be the conference proceedings issue due to be distributed at AWC in St John's. Umberto made an appeal to the Board for any suggestions of a reliable printing company that could be trusted with producing the physical journal going forward. There was some discussion about the technical standards to be met and the relevance of the physical location of the printer within Canada in terms of mailing, but basically any robust printing outfit should be capable of producing the journal. Some members of the Board suggested retaining a print management agency instead of dealing with a printing shop directly; they will provide information to Umberto.

8. Social Media Editor Report (Romain Dumoulin)

Jérémie shared the report that Romain submitted and went over some of the key points. The LinkedIn account is now followed by nearly 1000 members, an increase of 65 since the October meeting, and 7 new posts have been added since then. On Twitter we have 523 followers (an increase of 21) and a total of 239 tweets, of which 13 were added since the last meeting.

The content has been rather light on the job alert posts (only 2 out of the many more that are placed on the CAA web site); the intent is to have more of these replicated on social media. The publication of a new issue of Canadian Acoustics is always announced on social media, as are the awards conferred at each conference event. Also featured regularly in posts are events from the acoustics community and CAA local chapters.

9. Upcoming Meetings (reprise)

a. ISO TC43 Plenary Montréal 2023 (Jérémy Voix)

Jérémie gave a brief update; event will be hosted in May 2023 by ÉTS (École de technologie supérieure) in his university and preparations are well underway. The event will bring together the members of the TC43 standards subcommittees SC1 (Noise), SC2 (Building Acoustics) and SC3 (Underwater Acoustics) for a full week of meetings.

b. AWC 2023 / AWC 2024

No commitment has yet been made for either of these years. There was extensive discussion of potential locations. Niagara Falls was discussed as a potential target but a nearby seat of a university or centre of excellence would have to take the reins of organizing. Hamilton (McMaster; Live Lab) could fill that role; it will be explored by Bill and Andy. Jérémie pointed out that because of past experience, infrastructure and support it would be very easy to organize an AWC event in Montréal; he proposed therefore that Montréal host the conference in whichever of the two years is not selected for the event in Niagara Falls or other potential host location to be decided.

A further lengthy discussion took place on whether the traditional formula of the AWC being a physical event held yearly could be modified for a variety of reasons to a less frequent, or virtual, or hybrid, or alternating format. It was agreed to table the debate until after having had the experience of the first return to an in-person event in St. John’s, which will in some ways give proof of how willing delegates are to travel to a remote location to attend a physical conference.

c. Inter-noise 2025 - AWC 2025 Ottawa (Joana Rocha)

Joana gave a brief update. She has been working with a colleague at NRC on planning the bid for Inter-noise 2025 to be held in Ottawa. Ottawa and São Paulo, Brazil have been selected as runoff candidates by the Inter-noise committee and the formal proposal is being prepared for submission in July.

At this point there are two alternative outcomes. If Ottawa’s bid is successful, then the full focus of the organizing team will be on 2025 for a joint event combining Inter-noise and AWC. Should the city fail to secure Inter-noise, Joana would be willing to host AWC in Ottawa as a stand-alone conference in 2025 but could also consider holding it in 2024 if that year remains open at the time.

10. Varia

No new matters were raised.

11. Next Meeting

Agreed on a physical meeting on 27 September around 3 PM Newfoundland time in St. John’s for Board members attending AWC, with other members joining by video conference.

12. Motion to Adjourn

By Jérémie, at 4:28 PM Eastern time.


Solution
Problem
Cadna
ISO
17025

CANADIAN ACOUSTICS ANNOUNCEMENTS - ANNONCES TÉLÉGRAPHIQUES DE L'ACOUSTIQUE CANADIENNE

Looking for a job in Acoustics?

There are many job offers listed on the website of the Canadian Acoustical Association!

You can see them online, under http://www.caa-aca.ca/jobs/

August 5th 2015

Acoustic Training in Canada Database: Help us to help the younger generation and seasoned professionals

CAA is building a comprehensive list of all training programs offered in acoustics in Canada and we need your help! Below is a survey to help us populate that database that will eventually be available on CAA website. Please return all valuable input at your earliest convenience to Mr. DeGagne (wdegagne@caa-aca.ca)!

Dear CAA members, past members and friends, The purpose of this survey is to develop an online database of all the professional, undergraduate, and graduate acoustical courses and training programs offered through universities, colleges, associations, etc. This database would benefit the entire Canadian acoustic community in the following manner: 1. Track the different acoustical courses and training programs offered nationally 2. Allow CAA members to plan their acoustical training and easily select their perfect training program to meet their career aspirations 3. Allow CAA members to compare and contrast courses and training programs from different institutions 4. Allow institutions and the CAA to determine where the training gaps are and to plan for future programs demands To help us populate this database, simply return the following information at your earliest convenience to Mr. William DeGagne (wdegagne@caa-aca.ca), volunteer for CAA: 1. Place of the Course or Training program (university, colleges, etc.): 2. Name of Course or Training program: 3. Approx. date the Course or Training was followed: 4. Level (graduate, undergraduate, college course or professional training program, etc.): 5. Brief description of the Course or Training program: 6. Webpage of Course or Training program: 7. Location of Course or Training program (City, Province): 8. Course or Training program language: Thanks for you help towards the younger generation and seasoned professionals! :-)

May 31st 2021

24th International Congress on Acoustics (ICA 2022)

The 24th International Congress on Acoustics (ICA 2022) will be held at Hwabaek International Convention Center (HICO) in Gyeongju, Korea from October 24 to 28, 2022.

On behalf of the organizing committee, it is our great pleasure to invite you to the 24th International Congress on Acoustics, which will be held at Hwabaek International Convention Center (HICO) in Gyeongju, Korea from October 24 to 28, 2022. ICA2022 will offer the unique opportunity to learn about the study and latest researches as well as to exchange ideas and information on acoustics through plenary lectures, technical sessions, and poster Presentations. In addition, various social programs have been planned for participants to can enjoy the fascinating Korean culture and share our warm spirit of friendship. Koreans have a well-known love of music, from K-pop to Western classical music to reinterpretations of traditional Korean music. It follows then that Koreans are highly sensitive to the quality of sound, not only in musical instruments but also in everyday products and spaces. Thus our technical advancement in acoustics is tied to centuries of musical appreciation. As the cradle of the country's religion, philosophy, arts and of course, music, Gyeongju can offer visitors an insight into the development of acoustics in Korea. Furthermore, the entire city is an open-air museum full of ancient sites and treasures which include three UNESCO World Heritage Sites. In short, the unique and authentic glimpse of Korean culture through Gyeongju City into Korean culture makes it the ideal backdrop for ICA 2022. We look forward to seeing you in Gyeongju, Korea.

March 14th 2022

Acoustics Week in Canada 2022 (AWC22): Call for abstracts

Acoustics Week in Canada is happening in-person in St. John's, Newfoundland and Labrador from September 27-30

2022. The conference will take place at the Sheraton Hotel Newfoundland, and is being hosted by Dr. Len Zedel and Dr. Ben Zendel from Memorial University of Newfoundland. Submissions related to any aspect of acoustics are welcome until June 30th 2022 at https://awc.caa-aca.ca

Acoustics researchers, professionals, educators, and students are welcomed to St. John's for three days of plenary lectures and technical sessions from September 27-30 2022. The Canadian Acoustical Association Annual General Meeting will be held in conjunction with the conference, along the conference reception, the conference banquet (held at the provincial museum: The Rooms), and an exhibition of acoustical equipment and services. Participants will be able to take an acoustics tour of a ship in St. John's harbour, and a tour of the acoustics facilities at Memorial University. The conference will include a Harbour Symphony, where the music is made by the horns on ships in St. John's Harbour. And of course, participants will get to experience the hospitality and old world charm of downtown St. John's. We hope you will join us for Acoustics Week in Canada 2022 in St. John's Newfoundland and Labrador!
Abstract submissions are open until June 30th 2022, and registrations will open soon. Submissions related to any aspect of acoustics are welcome. For more information, visit https://awc.caa-aca.ca or contact the organizers at conference@caa-aca.ca

June 4th 2022

Acoustics Week in Canada 2022 (AWC22): Call for abstracts

Acoustics Week in Canada is happening in-person in St. John's, Newfoundland and Labrador from September 27-30 2022. The conference will take place at the Sheraton Hotel Newfoundland, and is being hosted by Dr. Len Zedel and Dr. Ben Zendel from Memorial University of Newfoundland. Submissions related to any aspect of acoustics are welcome until June 30th 2022 at https://awc.caa-aca.ca

Acoustics researchers, professionals, educators, and students are welcomed to St. John's for three days of plenary lectures and technical sessions from September 27-30 2022. The Canadian Acoustical Association Annual General Meeting will be held in conjunction with the conference, along the conference reception, the conference banquet (held at the provincial museum: The Rooms), and an exhibition of acoustical equipment and services. Participants will be able to take an acoustics tour of a ship in St. John's harbour, and a tour of the acoustics facilities at Memorial University. The conference will include a Harbour Symphony, where the music is made by the horns on ships in St. John's Harbour. And of course, participants will get to experience the hospitality and old world charm of downtown St. John's. We hope you will join us for Acoustics Week in Canada 2022 in St. John's Newfoundland and Labrador!
Abstract submissions are open until June 30th 2022, and registrations will open soon. Submissions related to any aspect of acoustics are welcome. For more information, visit https://awc.caa-aca.ca or contact the organizers at conference@caa-aca.ca

June 4th 2022

Acoustics Week in Canada 2022 (AWC22): Call for abstracts extended to July 15th!

Acoustics Week in Canada is happening in-person in St. John's, Newfoundland and Labrador from September 27-30 2022. The conference will take place at the Sheraton Hotel Newfoundland, and is being hosted by Dr. Len Zedel and Dr. Ben Zendel from Memorial University of Newfoundland. Submissions related to any aspect of acoustics are welcome now until July 15th 2022 at https://awc.caa-aca.ca

Please note that all authors will have to submit their 2-page article and pay their registration fees by August 1st (hard deadline) in order to have their proceedings paper published in the September issue of Canadian Acoustics (https://jcaa.caa-aca.ca). The authors are encouraged to use the available Microsoft™ Word or Latex templates.
For more information, visit https://awc.caa-aca.ca or contact the organizers at conference@caa-aca.ca

July 6th 2022

INTER-NOISE 2023 to be held August 20-23, 2023, in Makuhari Messe (Japan)

We are very pleased to inform you that the website of INTER-NOISE 2023 has been launched. Its link is https://internoise2023.org/.

The INTER-NOISE 2023 is held at Makuhari Messe (https://www.m-messe.co.jp/en/) from August 20-23, 2023, which is sponsored by International Institute of Noise Control Engineering (I-INCE) and is co-organized by Institute of Noise Control Engineering of Japan (INCE/J), Acoustical Society of Japan (ASJ).

August 12th 2022

À la recherche d'un emploi en acoustique ?

De nombreuses offre d'emploi sont affichées sur le site de l'Association canadienne d'acoustique !

Vous pouvez les consulter en ligne à l'adresse http://www.caa-aca.ca/jobs/

August 5th 2015

Répertoire des formations en acoustique au Canada : aidez-nous à aider la jeune génération et nos professionels d'expérience

L'ACA est en train de dresser une liste complète de tous les programmes de formation offerts en acoustique au Canada et nous avons besoin de votre aide ! Vous trouverez ci-dessous un sondage qui nous aidera à alimenter cette base de données qui sera éventuellement disponible sur le site Web de la CAA. Veuillez retourner vos précieux commentaires à M. DeGagne (wdegagne@caa-aca.ca) dans les plus brefs délais !

Chers membres, anciens membres et amis de l'ACA, Le but de cette enquête est de développer une base de données en ligne de tous les cours et programmes de formation en acoustique professionnels, de premier et de deuxième cycle, offerts par les universités, les collèges, les associations, etc. Cette base de données profiterait à l'ensemble de la communauté acoustique canadienne de la manière suivante : 1. Suivre les différents cours et programmes de formation en acoustique offerts à l'échelle nationale. 2. Permettre aux membres de l'ACA de planifier leur formation en acoustique et de choisir facilement le programme de formation idéal pour répondre à leurs aspirations professionnelles. 3. Permettre aux membres de l'ACA de comparer et d'opposer les cours et les programmes de formation de différentes institutions. 4. Permettre aux institutions et à l'ACA de déterminer où se trouvent les lacunes en matière de formation et de planifier les demandes de programmes futurs. Pour nous aider à alimenter cette base de données, il vous suffit de retourner les informations suivantes dans les meilleurs délais à M. William DeGagne (wdegagne@caa-aca.ca), bénévole pour l'ACA : 1. Lieu du cours ou du programme de formation (université, collèges, etc.) : 2. Nom du cours ou du programme de formation : 3. Date approximative à laquelle le cours ou la formation a été suivi. 4 : 4. Niveau (études supérieures, premier cycle, cours collégial ou programme de formation professionnelle, etc :) 5. Brève description du cours ou du programme de formation : 6. Page web du cours ou du programme de formation : 7. Lieu du cours ou du programme de formation (ville, province) : 8. Langue du cours ou du programme de formation : Merci pour votre aide à l'intention de la jeune génération et de nos professionels d'expérience ! :-)

May 31st 2021

Semaine canadienne de l'acoustique (AWC22): Appel à résumés

La Semaine canadienne de l'acoustique se déroulera en personne à St. John's, Terre-Neuve-et-Labrador, du 27 au 30 septembre 2022. La conférence aura lieu au Sheraton Hotel Newfoundland et sera organisée par le Dr Len Zedel et le Dr Ben Zendel de l'Université Memorial de Terre-Neuve. Les soumissions relatives à tout aspect de l'acoustique sont les bienvenues jusqu'au 30 juin 2022 à l'adresse https://awc.caa-aca.ca

Les chercheurs, professionnels, éducateurs et étudiants en acoustique sont les bienvenus à St. John's pour trois jours de conférences plénières et de sessions techniques du 27 au 30 septembre 2022. L'assemblée générale annuelle de l'Association canadienne d'acoustique aura lieu en même temps que la conférence, ainsi que la réception de la conférence, le banquet de la conférence (qui se tiendra au musée provincial : The Rooms) et une exposition d'équipements et de services acoustiques. Les participants pourront faire une visite acoustique d'un navire dans le port de St. John's, et une visite des installations acoustiques de l'Université Memorial. La conférence comprendra une symphonie portuaire, au cours de laquelle la musique sera jouée par les sirènes des navires dans le port de St. John's. Et bien sûr, les participants auront l'occasion de découvrir l'hospitalité et le charme du vieux monde du centre-ville de St. John's. Nous espérons que vous vous joindrez à nous pour la Semaine canadienne de l'acoustique 2022 à St. John's, Terre-Neuve et Labrador ! Les soumissions de résumés sont ouvertes jusqu'au 30 juin 2022, et les inscriptions seront bientôt ouvertes. Les soumissions liées à tous les domaines de l'acoustique sont les bienvenues. Pour plus d'informations, visitez https://awc.caa-aca.ca ou contactez les organisateurs à conference@caa-aca.ca .

June 4th 2022

Semaine canadienne de l'acoustique (AWC22): Appel à résumés

La Semaine canadienne de l'acoustique se déroulera en personne à St. John's, Terre-Neuve-et-Labrador, du 27 au 30 septembre 2022. La conférence aura lieu au Sheraton Hotel Newfoundland et sera organisée par le Dr Len Zedel et le Dr Ben Zendel de l'Université Memorial de Terre-Neuve. Les soumissions relatives à tout aspect de l'acoustique sont les bienvenues jusqu'au 30 juin 2022 à l'adresse https://awc.caa-aca.ca

Les chercheurs, professionnels, éducateurs et étudiants en acoustique sont les bienvenus à St. John's pour trois jours de conférences plénières et de sessions techniques du 27 au 30 septembre 2022. L'assemblée générale annuelle de l'Association canadienne d'acoustique aura lieu en même temps que la conférence, ainsi que la réception de la conférence, le banquet de la conférence (qui se tiendra au musée provincial : The Rooms) et une exposition d'équipements et de services acoustiques. Les participants pourront faire une visite acoustique d'un navire dans le port de St. John's, et une visite des installations acoustiques de l'Université Memorial. La conférence comprendra une symphonie portuaire, au cours de laquelle la musique sera jouée par les sirènes des navires dans le port de St. John's. Et bien sûr, les participants auront l'occasion de découvrir l'hospitalité et le charme du vieux monde du centre-ville de St. John's. Nous espérons que vous vous joindrez à nous pour la Semaine canadienne de l'acoustique 2022 à St. John's, Terre-Neuve et Labrador ! Les soumissions de résumés sont ouvertes jusqu'au 30 juin 2022, et les inscriptions seront bientôt ouvertes. Les soumissions liées à tous les domaines de l'acoustique sont les bienvenues. Pour plus d'informations, visitez https://awc.caa-aca.ca ou contactez les organisateurs à conference@caa-aca.ca .

June 4th 2022

Semaine canadienne de l'acoustique (AWC22): Appel à résumés reporté au 15 juillet!

La Semaine canadienne de l'acoustique se déroulera en personne à St. John's, Terre-Neuve-et-Labrador, du 27 au 30 septembre 2022. La conférence aura lieu au Sheraton Hotel Newfoundland et sera organisée par le Dr Len Zedel et le Dr Ben Zendel de l'Université Memorial de Terre-Neuve. Les soumissions de résumés sont ouvertes jusqu'au 15 juillet 2022 sur le site https://awc.caa-aca.ca.

Veuillez noter que tous les auteurs devront soumettre leur article de 2 pages et payer leurs frais d'inscription avant le 1er août (date limite immuable) afin que leur article soit publié dans le numéro de septembre de Canadian Acoustics (https://jcaa.caa-aca.ca). Les auteurs sont encouragés à utiliser les gabarits Microsoft™ Word ou LaTex disponibles. Pour plus d'informations, visitez https://awc.caa-aca.ca ou contactez les organisateurs à conference@caa-aca.ca .

July 6th 2022

Why publish in Canadian Acoustics?

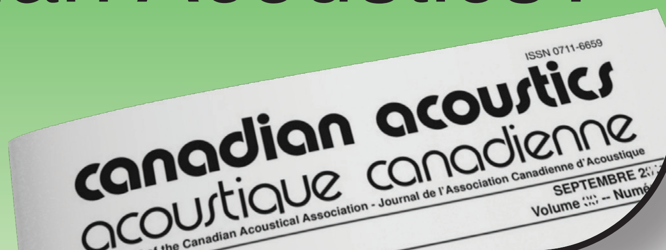

Because, it is...

- A respected scientific journal with a 40-year history uniquely dedicated to acoustics in Canada
- A quarterly publication in both electronic and hard-copy format, reaching a large community of experts worldwide
- An Open Access journal, with content freely available to all, 12 months from time of publication
- A better solution for fast and professional review providing authors with an efficient, fair, and constructive peer review process.

Pourquoi publier dans Acoustique canadienne ?

Parce que, c'est...

- Une revue respectée, forte de 40 années de publications uniquement dédiée à l'acoustique au Canada

- Une publication trimestrielle en format papier et électronique, rejoignant une large communauté d'experts à travers le monde

- Une publication "accès libre" dont le contenu est disponible à tous, 12 mois après publication

- Une alternative intéressante pour une évaluation par les pairs, fournissant aux auteurs des commentaires pertinents, objectifs et constructifs

Application for Membership

CAA membership is open to all individuals who have an interest in acoustics. Annual dues total $120.00 for individual members and $50.00 for student members. This includes a subscription to ***Canadian Acoustics***, the journal of the Association, which is published 4 times/year, and voting privileges at the Annual General Meeting.

Subscriptions to *Canadian Acoustics* *or* Sustaining Subscriptions

Subscriptions to ***Canadian Acoustics*** are available to companies and institutions at a cost of $120.00 per year. Many organizations choose to become benefactors of the CAA by contributing as Sustaining Subscribers, paying $475.00 per year (no voting privileges at AGM). The list of Sustaining Subscribers is published in each issue of ***Canadian Acoustics*** and on the CAA website.

Please note that online payments will be accepted at http://jcaa.caa-aca.ca

Address for subscription / membership correspondence:

Name / Organization ______________________________

Address ______________________________

City/Province ______________ Postal Code ________ Country ______________

Phone ______________ Fax ______________ E-mail ______________

Address for mailing Canadian Acoustics, if different from above:

Name / Organization ______________________________

Address ______________________________

City/Province ______________ Postal Code ________ Country ______________

Areas of Interest: (Please mark 3 maximum)

1. Architectural Acoustics
2. Engineering Acoustics / Noise Control
3. Physical Acoustics / Ultrasound
4. Musical Acoustics / Electro-acoustics
5. Psychological / Physiological Acoustic
6. Shock and Vibration
7. Hearing Sciences
8. Speech Sciences
9. Underwater Acoustics
10. Signal Processing / Numerical Methods
11. Other

For student membership, please also provide:

__________ __________ ____________________ __________

(University) *(Faculty Member)* *(Signature of Faculty Member)* *(Date)*

I have enclosed the indicated payment for:
[ ] CAA Membership $ 120.00
[ ] CAA Student Membership $ 50.00

Corporate Subscriptions (4 issues/yr)
[ ] $120 including mailing in Canada
[ ] $128 including mailing to USA,
[ ] $135 including International mailing

[ ] Sustaining Subscription $475.00
(4 issues/yr)

Please note that the preferred method of payment is by credit card, online at http://jcaa.caa-aca.ca

For individuals or organizations wishing to pay by check, please register online at *http://jcaa.caa-aca.ca* and then mail your check to:

Executive Secretary, Canadian Acoustical:
Dr. Roberto Racca
c/o JASCO Applied Sciences
2305–4464 Markham Street
Victoria, BC V8Z 7X8 Canada

Formulaire d'adhésion

L'adhésion à l'ACA est ouverte à tous ceux qui s'intéressent à l'acoustique. La cotisation annuelle est de 120.00$ pour les membres individuels, et de 50.00$ pour les étudiants. Tous les membres reçoivent ***l'Acoustique Canadienne***, la revue de l'association.

Abonnement pour la revue *Acoustique Canadienne* et abonnement de soutien

Les abonnements pour la revue ***Acoustique Canadienne*** sont disponibles pour les compagnies et autres établissements au coût annuel de 120.00$. Des compagnies et établissements préfèrent souvent la cotisation de membre bienfaiteur, de 475.00$ par année, pour assister financièrement l'ACA. La liste des membres bienfaiteurs est publiée dans chaque issue de la revue ***Acoustique Canadienne***..

Notez que tous les paiements électroniques sont acceptés en ligne http://jcaa.caa-aca.ca

Pour correspondance administrative et financière:

Nom / Organisation ______________________________

Adresse ______________________________

Ville/Province ______________ Code postal__________ Pays ______________

Téléphone ______________ Téléc. ______________ Courriel ______________

Adresse postale pour la revue Acoustique Canadienne

Nom / Organisation ______________________________

Adresse ______________________________

Ville/Province ______________ Code postal__________ Pays ______________

Cocher vos champs d'intérêt: (maximum 3)

1. Acoustique architecturale
2. Génie acoustique / Contrôle du bruit
3. Acoustique physique / Ultrasons
4. Acoustique musicale / Électro-acoustique
5. Physio / Psycho-acoustique
6. Chocs et vibrations
7. Audition
8. Parole
9. Acoustique sous-marine
10. Traitement des signaux /Méthodes numériques
11. Autre

Prière de remplir pour les étudiants et étudiantes:

__________ __________ __________ __________

(Université) (Nom d'un membre du corps professoral) (Signature du membre du corps professoral) (Date)

Cocher la case appropriée:
[ ] Membre individuel 120.00 $
[ ] Membre étudiant(e) 50.00 $

Abonnement institutionnel
[ ] 120 $ à l'intérieur du Canada
[ ] 128 $ vers les États-Unis
[ ] 135 $ tout autre envoi international

[ ] Abonnement de soutien 475.00 $ (comprend l'abonnement à *L'acoustique Canadienne*)

Merci de noter que le moyen de paiement privilégie est le paiement par carte crédit en ligne à *http://jcaa.caa-aca.ca*

Pour les individus ou les organisations qui préféreraient payer par chèque, l'inscription se fait en ligne à *http://jcaa.caa-aca.ca* puis le chèque peut être envoyé à :

Secrétaire exécutif, Association canadienne d'acoustique :
Dr. Roberto Racca
c/o JASCO Applied Sciences
2305–4464 Markham Street
Victoria, BC V8Z 7X8 Canada

Canadian Acoustical Association
Association canadienne d'acoustique

Board of Directors - Conseil d'administration

SUSTAINING SUBSCRIBERS - ABONNÉS DE SOUTIEN

The Canadian Acoustical Association gratefully acknowledges the financial assistance of the Sustaining Subscribers listed below. Their annual donations (of $475 or more) enable the journal to be distributed to all at a reasonable cost.
L'Association Canadienne d'Acoustique tient à témoigner sa reconnaissance à l'égard de ses Abonnés de Soutien en publiant ci-dessous leur nom et leur adresse. En amortissants les coûts de publication et de distribution, les dons annuels (de 475$ et plus) rendent le journal accessible à tous les membres.

Acoustec Inc.
Jean-Philippe Migneron - 418-496-6600
info@acoustec.qc.ca
acoustec.qc.ca

Acoustex Specialty Products
Mr. Brian Obratoski - 2893895564
Brian@acoustex.ca
www.acoustex.net

AcoustiGuard-Wilrep Ltd.
Mr. William T. Wilkinson - 888-625-8944
wtw@wilrep.com
acoustiguard.com

AECOM
Alan Oldfield - 9057127058
alan.oldfield@aecom.com
aecom.com

Aercoustics Engineering Ltd.
Nicholas Sylvestre-Williams - (416) 249-3361
NicholasS@aercoustics.com
aercoustics.com

Audio Precision (c/o GerrAudio Distribution in Canada)
Peter Snelgrove -
peter@gerr.com
www.gerr.com

Dalimar Instruments Inc
Monsieur Daniel Larose - 450-424-0033
daniel@dalimar.ca
www.dalimar.ca

dB Noise Reduction
Mehrzad Salkhordeh - 519-651-3330 x 220
mehrzad@dbnoisereduction.com
dbnoisereduction.com

GRAS Sound & Vibration (c/o GerrAudio Distribution in Canada)
Peter Snelgrove -
peter@gerr.com
www.gerr.com

HGC Engineering Ltd.
Mr. Bill Gastmeier -
bill@gastmeier.ca
hgcengineering.com

Hottinger Bruel & Kjaer inc.
Andrew Khoury - 514-695-8225
andrew.khoury@hbkworld.com
bksv.com

Integral DX Engineering Ltd.
Gregory Clunis - 613-761-1565
greg@integraldxengineering.ca
integraldxengineering.ca

Jade Acoustics Inc.
Ms. Dalila Giusti - 905-660-2444
dalila@jadeacoustics.com
jadeacoustics.com

JASCO Applied Sciences (Canada) Ltd.
Roberto Racca - +1.250.483.3300 ext.2001
roberto.racca@jasco.com
www.jasco.com

Pyrok Inc.
Howard Podolsky - 914-777-7770
mrpyrok@aol.com
pyrok.com

RWDI
Mr. Peter VanDelden - 519-823-1311
peter.vandelden@rwdi.com
rwdi.com

Scantek Inc.
Edward Okorn -
E.Okorn@ScantekInc.com
scantekinc.com

Soft dB Inc.
Dr. Roderick Mackenzie - 5148056734
r.mackenzie@softdb.com
softdb.com

Xprt Integration
Mr. Rob W Sunderland - 604-985-9778
rob@xprt.ca